— G4978—

HOLOGRAPHIC METHODS IN THE STUDIES OF THIN FILM STRESS, VIBRATION ANALYSIS AND PATTERN RECOGNITION

A THESIS
SUBMITTED IN PARTIAL FULFILMENT OF
THE REQUIREMENT FOR THE DEGREE OF
DOCTOR OF PHILOSOPHY

BY
P. T. AJITH KUMAR

DEPARTMENT OF PHYSICS
COCHIN UNIVERSITY OF SCIENCE AND TECHNOLOGY
COCHIN - 682 022
INDIA

FEBRUARY 1991

CERTIFICATE

Certified that the work reported in this thesis is based on the bonafide work done by Mr. Ajith Kumar P.T, under my guidance in the Department of Physics, Cochin University of Science and Technology and has not been included in any other thesis submitted previously for the award of any degree.

C. Purushothaman

Cochin 682 022

05-02-1991

Prof. C. Purushothaman

(Supervising Teacher)

CONTENTS

LIST OF FIGURES

PREFACE

The birth of a new area in modern optics took place when,in 1948,Dennis Gabor, the Hungarian physicist conceived the idea of wave front reconstruction . But it was the advent of Lasers in 1960 which impelled the growth of this new technique named Holography. Holography emerged as a faithful form of photography to render the life - like 3-D images. As it stands now it is more a scientific search tool whose applications are as diverse as imaging, information storage and processing, non-destructive testing, vibration analysis, microscopy, road flatness testing and identification of target objects.

This thesis documents the details of fabrication of an indigenous holographic setup and the results of some experimental research done by using it.All the components of the setup except the laser and lenses were fabricated in the department. The methods used for the fabrication of spatial filters, beam splitters,beam directors and other system components are also presented.

The initial part of the work is the study on the isolation capability of a newly designed low cost holographic table. The design details of the table and the essential vibration characteristics are discussed.It is seen, by comparison with commercial data, that the overall performance of this table is comparable to that of the ordinary honeycomb structures without internal damping.

The studies conducted are mainly on Holographic Interferometry (HI) and Holographic Optical Elements (HOEs). The HI part consists of real-time and time-averaged studies . A new non-destructive method for the study of thermal stress in thin films has been introduced and tested. Both diffusely and specularly reflecting films were used.

Time-averaged holographic interferometry has been generally applied for the vibration analysis of musical stringed instruments. But the use of this technique is limited in the case of musical wind instruments, due to problems of stability during excitation. We have made an attempt to record the vibration pattern of an air-reed wind instrument excited in an almost realistic way. It has been shown that well defined time-averaged interferograms can be obtained in the case of a wind instrument.

Different holographic optical elements were recorded using the setup and an optical pattern recognition system using HOEs has been fabricated and optimized.

The contents of the thesis are presented in six chapters.

An overview of the growth of holography and the necessary theory are given in the first chapter.

The second chapter discusses the experimental setup, fabrication details of the various system components and the preliminary experiments done.Vibration analysis of the low cost holographic table is also presented in this chapter.

The *in-situ* processing of the holograms and the real-time monitoring of the thermal stress in thin films, its measurements and the studies conducted in this area are given in the third chapter.

The fourth chapter is concerned with the experimental setup for the excitation of an air-reed musical wind instrument in an almost realistic playing condition and without introducing any stability problem. The time-averaged holographic interferograms obtained for the Indian flutes that we have used, are also presented.

Holographic optical elements and the development of a holographic pattern recognition system form the theme of the fifth chapter. Finally, the summary of the investigations done and the contributions of the work are listed.

Most of the conclusions drawn through this research work have been published/ accepted /communicated for publication/presented in seminars,in the form of the following papers.

1. **" A New Design for a Holographic Table ",**
   P.T,Ajith Kumar, E.M.S.Nair and C.Purushothaman,
   J. Phys. E., Sci. Instrum. 19, (1986), p 643, BRITAIN.
2. **" A New Method for the Study of Vibrations of Air-Reed Wind Instruments by using Holography ",**
   P.T.Ajith Kumar, Jessy P. Thomas and C. Purushothaman,
   Presented in the " National Symposium on Current Trends in pure and Applied Physics",
   Dept. of Physics, CUSAT,COCHIN-22, Oct:24-25, (1988).
3. **".A Holographic Method for the Study of Thermal Stress in Thin Films ",**
   P.T.Ajith Kumar and C.Purushothaman,
   "Proc.of the International Workshop on Holography and Speckle Phenomena and their Industrial Applications.",
   R.S.Sirohi (Ed),World Scientific, SINGAPORE, p 161." Indian Institute of Technology ", MADRAS, Dec:12-17 (1988).

4. " A Live Fringe Technique for Stress Measurements in Reflecting Thin Films by using Holography ",
   P.T.Ajith Kumar and C.Purushothaman,
   Optics and Laser Technology, 22, 2841, (1990), ENGLAND.
5. " Some Studies on Fabrication of Optical Elements, Stress in Thin Films and Vibrations of Air-Reed Wind Instruments, by using holography " ,
   P.T.Ajith Kumar and C.Purushothaman,
   First Kerala Science Congress, CUSAT, COCHIN-22, Feb:(1989).
6. "Vibrations of Flutes Studied by Holographic Interferometry"
   P.T.Ajith Kumar and C.Purushothaman,
   " National Symposium on Acoustics",
   Sangeeth Research Academy, Dec: 14-16, (1989), CALCUTTA,
   Also in J.Acoust.Soc.Ind. 17,343, (1989).
7. " Study of Flute Vibrations by Holographic Interferometry ",
   P.T.Ajith Kumar, Jessy P. Thomas and C.Purushothaman,
   Appl. Opt.29, 2841, (1990),USA.
8. "Study of Thermal Stress in Thin Films by Real-Time Holographic Interferometry " (Accepted),
   Sixth International PRECISION ENGINEERING Seminar,May:27-31,(1991), Stadthalle,GERMANY,
9. " Surface Vibrations of Musical Wind Instruments ",
   J. Acoust. Soc. Am.,USA, (Communicated).
10. " Thermal Stress Variation in Reflecting Thin Films studied by Holographic Interferometry "
    Thin Solid Films,NETHERLANDS,(Communicated).

CHAPTER I

INTRODUCTION

INTRODUCTION

1.1 Overview of Holography

Man can perceive the light distribution and actual shape of any illuminated object, through his eyes. But almost all light sensitive materials in nature respond only to irradiance. As a result when we try to record an image in such materials, what we get is merely the intensity distribution of the seen. All information about the three dimensional shape or in other words, information about the relative phases of the light waves coming from different points of the object is lost.

Holography is a way of recording and reproducing waves with both the amplitude and phase details. The waves may be light,sound or 'corpuscular'.The basic principles of this type of imaging can be traced back to the work done by Wolfke[1] and Bragg[2,3] in x-ray crystallography. But it was Dennis Gabor [4,6] who conceived the idea of holographic imaging in 1948. The technique was invented as a two-step coherent imaging process with the specific application of high resolution electron microscopy in mind. The word Hologram originates from the Greek 'Holos' meaning complete and 'Gram' meaning information [7].

In Gabor's original method, called on-axis holography, the actual reconstructed image was superposed on a conjugate image and the scattered background light. In addition

to this problem of twin-image and dc, the non-availability of highly coherent and powerful sources of light stood against the progress of Holography.

With the advent of laser [8] in 1960, another breakthrough in the technique of recording Hologram was achieved through the introduction of off-axis holography by Leith and Upatnieks [9-11] in 1962. Using this technique it is possible to separate in space,the components of the reconstructed wave viz. the real, the virtual and the dc and thus avoids the drawbacks of Gabor's holography. Leith and Upatnieks also pointed out the possibility of multicolour image production [12].

Another important advance in the field was independently reported by the Russian scientist Denisyuk [13-15] who used reflected light to record holograms.

The availability of lasers, off-axis technique and development of new recording materials with high efficiency gave great impetus to holography and set off an explosive increase in its scientific applications.

In 1964 pulsed ruby laser was used by Silverman et al.[16] to record spectacular life-size hologram and portraits. Far-field holography developed by Thompson and Parrent [17,18] emerged as one of the first direct applications of holography ie. particle size analysis. Optical information storage in solids [19,20], character recognition by matched filtering [21], image processing [22], high resolution imaging

of aerosols [23] and imaging though diffusing media [24,25] are some other initial applications. The most salient of these applications was holographic interferometry [26-30] and holographic optical elements [31-33]. A detailed account of these are presented in chapters III and V respectively.

The invention of rainbow holography by Benton [34], non-coherent light holography by Chang [35], multiplex holography by Cross [36], and the possibility of replication made this scientist's search tool inexpensive and a layman's fancy item popular now in commercial market. In 1979 Huignard et al. [37] used real-time holography to generate phase-conjugate wave fronts from Bi_{12} SiO_{20} crystals. The use of digital computers for the production of holograms [38-40] introduced a new wave of interest. A micro-computer system has been used by P.Hariharan et al. [41] to produce holographic interferograms and there by to measure small vector displacements.

Many people were drawn to the fascinating world of holography and it has been extensively and effectively applied to numerous areas. For some it is a nicety, for others the incentive is its truly successful commercial value, but for many it is a valuable contrivance for scientific and engineering studies for which it is uniquely suited.

1.2 Technique of Holography

A Hologram is a record of an interference pattern formed between two fields.When this record of interference pattern is 'illuminated' with a beam equivalent to any one of

the interfering beams, the other field is exactly re-created.If one field carries information about an object of interest, then the second field is a coherent, reproducible reference. Both the amplitude and phase of the field are stored and re-created,because the intensity at any point in the interference pattern depends on the phase as well as the amplitude. Since all the recording media are square law detectors ie. they respond only to the intensity, all the phase information of the waves are converted to variations of intensity. The resultant image will look so live as if the observer sees the object through a window whose size is that of the hologram. The basic theory and requirements for holographic recording are discussed below .

1.2.1 Two beam interference

Consider two point sources S_1 and S_1 in an isotropic medium. Assume that the waves are polarized in one plane, the electric vector perpendicular to the plane of the paper, and have the same frequency ν. The light oscillations at any arbitrary point 'P' can be written as

$$x_1 = A_1\cos(\omega t+\phi_1) \qquad (1.1)$$

$$x_2 = A_2\cos(\omega t+\phi_2) \qquad (1.2).$$

A_1 and A_2 are the amplitudes of the waves, ω the angular frequency ($2\pi\nu$) and ϕ = initial phase $-\frac{2\pi r}{\lambda}$, where r is the distance of the point P from the source (Fig.1.1)

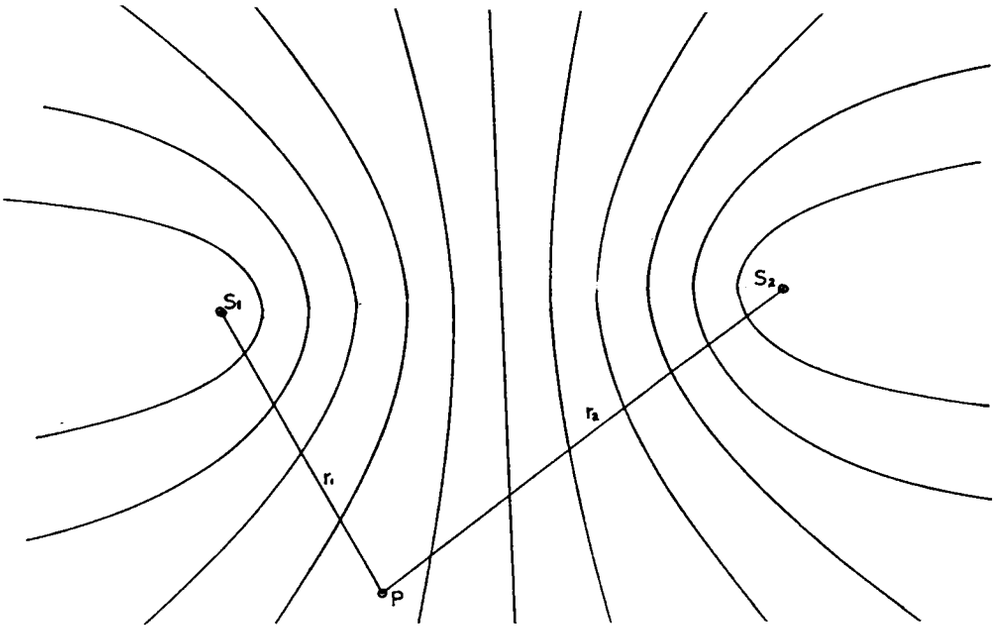

Fig.1.1 System of hyperboloids in the region of interference

The resultant oscillation at point P can be written as

$$x = A_1\cos(\omega t+\phi_1) + A_2\cos(\omega t+\phi_2)$$

$$= A\cos(\omega t+\phi) \qquad (1.3)$$

where $A^2 = A_1^2 + A_2^2 + 2A_1A_2\cos(\phi_1 - \phi_2)$ (1.4)

and $$\phi = \tan^{-1}\left[\frac{A_1\mathrm{Sin}(\phi_1) + A_2\,\mathrm{Sin}(\phi_2)}{A_1\mathrm{Cos}(\phi_1) + A_2\,\mathrm{Cos}(\phi_2)}\right] \qquad (1.5)$$

Since the exposure time is very much greater than the oscillation period of light, the mean value of intensity is always recorded. If the sources S_1 and S_2 are mutually independent (incoherent) then the mean value of $\mathrm{Cos}(\phi)$ during this recording time will be zero and then (1.4) becomes

$$A^2 = A_1^2 + A_2^2 \qquad (1.6)$$

If the difference in initial phases does not change in time (coherent), the effect is different. Consider the in phase and anti-phase conditions ie.

$$\phi_1 - \phi_2 = 0, \pm 2\pi, \ldots\ldots, \pm 2n\pi \qquad (1.7)$$

$$\phi_1 - \phi_2 = \pm\pi, \pm 3\pi \ldots\ldots, \pm(2n+1)\pi \qquad (1.8)$$

n is any integer. We can write (1.4) as

$$A^2 = A_1^2 + A_2^2 \pm 2A_1A_2$$

or $$A = A_1 + A_2 \qquad (1.9)$$

and $$A = A_1 - A_2 \qquad (1.10)$$

(1.6),(1.9) and (1.10) implies that in incoherent illumination the intensities of the sources are added and in coherent illumination the amplitudes are added. Thus in the region of interference a set of maximum and minimum disturbance surfaces are formed. If the initial phases are zeros, the anti node surface condition (1.7) takes the form

$$r_1 - r_2 = \pm n\lambda \qquad (1.11)$$

which represents a system of hyperboloids (Fig.1.1) with the axis of rotation S_1S_2.From (1.7) it is also clear that there are 2n+1 anti nodal surfaces in between the sources. If s is the distance between the sources, the maximum value of $r_1 - r_2$ does not exceed s. Maximum value of n ie. $n_{max} = s/\lambda$ and the total number of anti nodal hyperboloids is $(2s/\lambda)+1$. The planes tangential to the surfaces of the nodes or anti nodes at each point bisect the angle 2α between the vectors $r_1$and r_2. The spacing d between the adjacent hyperboloids will be minimum along S_1S_2 and will be equal to $\lambda/2$. In the general case $d = \lambda/2 \sin(\alpha)$ and spatial frequency

$$f = 2 \sin(\alpha)/\lambda \qquad (1.12)$$

as the angle between the waves increases, the spacing decreases.

1.2.2 Recording media and other basic requirements

If a material is to be used for holographic recording,it must respond to light with a spatial modulation of absorption,refractive index or thickness.An ideal recording medium requires macroscopic properties such as low exposure sensitivity,high resolving power,long storage time and recyclability.If ρ lines/mm is the resolving power of the recording material,holography requires (1.12) that $1/\rho \leq d$. Some of the popular recording media are photo emulsions,dichromated gelatin,photo resist,photo polymers,photo plastics and photo chromics .The materials are mainly classified as `absorption 'and `phasematerials '.In an absorption material,fringes are recorded as a spatial variation of its light absorption.Silver halide emulsion, photochromatic glasses and plastics come under this type.

If the recording is `linear' the irradiance variation before processing are linearly recorded as transmittance variations after processing. The light amplitude transmittance of the processed hologram can then be written as

$$T = \frac{\text{amplitude transmitted}}{\text{amplitude incident}} = T_0 - \beta\tau I \qquad (1.13)$$

where T_0 is the transmittance of the unexposed plate, β is a constant depending on the emulsion type and the processing, τ is the exposure time and I the intensity.

In a phase material the spatial modulations are either that of refractive index or that of thickness.

In a microscopic scale the response of the above

materials can be described by curves of amplitude transmittance or effective phase shift versus exposure. In practice the actual modulation of fringe intensity within the recording material is always less than that of the original interference pattern.This is because of lateral spreading of light within the medium due to scattering. For a particular spatial frequency,the ratio of actual modulation to the input modulation is termed as modulation transfer function (MTF).

The diffraction efficiency of a hologram, defined as the ratio of the energy diffracted into the desired image to that illuminating the hologram, is another parameter characterizing the recording material. A material is taken as more sensitive if, for fixed illumination conditions, less exposure is required to record a hologram of specified diffraction efficiency.

About the light source, the coherent length of the source must be equal to or greater than the maximum difference in the object and reference beam path lengths .Gas lasers offer the highest coherence length.Since the recording process is photography of an interference pattern, during the exposure anything in the entire setup must not be permitted to move more than a quarter wave length. Ground vibrations and vibrations of the work-surface, air currents, acoustic waves and temperature fluctuations have to be minimized to prevent obliteration of the interference fringes.

For best results the total distance travelled by the reference and object beams from the beam splitter to the hologram plane should be nearly equal.The dimensions of the

object must be compatiable with the lateral and longitudinal coherent distances of the laser source. Beam ratio and angle between the beams should be properly chosen. Above all, the room should be dust free,humidity controlled and contamination of air is to be eliminated.

1.2.3 Wave front reconstruction

When a hologram is illuminated by the reference beam or a wave similar to the reference beam, the microscopic fringes in the hologram diffract the wave and a part of the wave diffracted out of this illuminating beam is directed and shaped by the hologram into a 're-construction' of the original object wave. An observer will perceive a virtual image of the object located exactly at the actual object position .On the other hand if the reference beam is precisely retroreflected to illuminate the back side of the hologram, a real image of the object is produced at the original object location.

Let O and R represent the complex amplitudes of the object wave and reference wave,respectively. The interference pattern that results due to the mixing of these two waves is recorded on a high spatial resolution photographic emulsion. For the sake of simplicity assume plane absorption holograms, then intensity distribution can be expressed as

$$I(x,y) = (O+R)(O+R)^{*}$$
$$= |O|^{2} + |R|^{2} + OR^{*} + O^{*}R \qquad (1.14),$$

* denotes the complex conjugate.

Assume that the complex amplitude of the object wave at the

hologram plane is weak compared to that of the reference wave, ie. $|O(x,y)| << |R(x,y)|$, which is the most common case.

Assume that the recording is linear and the transparency, (hologram) after processing possesses a transmittance governed by (1.13).When the hologram is illuminated with the reference wave, the reconstructed field at the hologram plane is given by

$$\psi(x,y) = R(x,y)\, T(x,y) \qquad (1.15)$$

$$= R(x,y)\left[T_0 - \beta\tau I(x,y)\right]$$

$$= R(x,y)\, T_0 - \beta\tau |R|^2 R(x,y) - \beta\tau\, |O|^2 R(x,y)$$

$$- \beta\tau |R|^2 O(x,y) - \beta\tau\, O^*(x,y) R^2(x,y) \qquad (1.16)$$

The first three terms in the above equation is the direct wave which consist of the attenuated reference beam and spatially varying halo due to the second term. The third term is extremely small in comparison to other terms, since it has been assumed that $|O(x,y)| << |R(x,y)|$.The fourth term is same as the original object wave, except for a constant factor and forms the virtual image. In the off-axis (Leith and Upatnieks) hologram,this wave is separated from the rest. In the same way the fifth term corresponds to a wave which resembles the object wave, except that it is of opposite curvature and converges to the conjugate real image, which is deflected off the axis at an angle nearly twice that which the reference wave makes with it (Fig.1.2).The image is psudoscopic. A hologram has the associative property and can be reconstructed with any of the interfering waves.

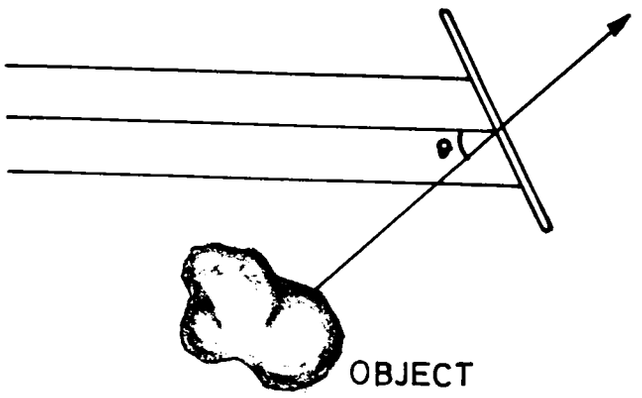

Fig.1.2. Off-axis recording and reconstruction.

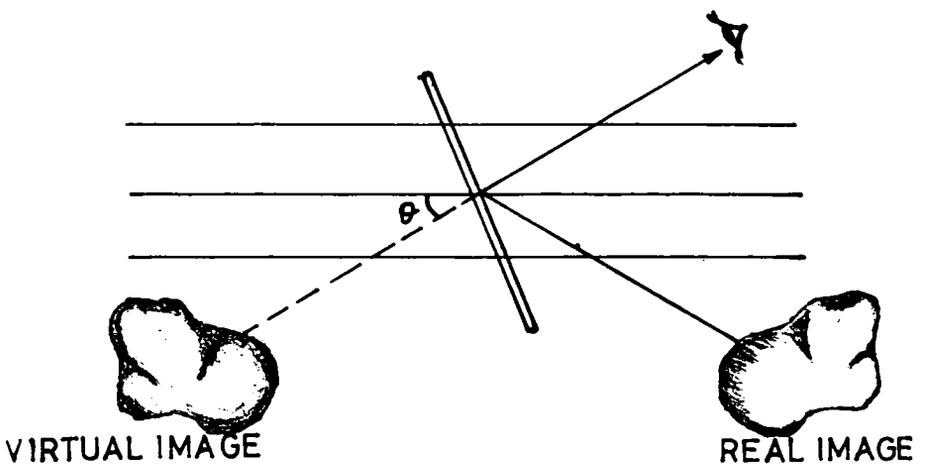

References

1. Wolfke M,(1920),Physikalische Zeitschrift,21,425.

2. Bragg W.L,(1939),Nature,143,678.

3. Bragg W.L,(1942),Nature,149,470.

4. Gabor D,(1948),Nature,161,777.

5. Gabor D,(1949),Proc.Royal Soc.A,197,454.

6. Gabor D,(1951),Proc.Phys Soc.B,64,449.

7. Gabor D,(1972),Proc.IEEE.60,655.

8. Maiman T.H,(1960),Nature,187,493.

9. Leith E.N and Upatnieks J.(1962),J.Opt.Soc.Am,52,1123.

10. Leith E.N and Upatnieks J.(1963),J.Opt.Soc.Am,53,1377.

11. Leith E.N and Upatnieks J.(1965),J.Opt.Soc.Am,55,569.

12. Leith E.N and Upatnieks J.(1964),J.Opt.Soc.Am,54,1295.

13. Denisyuk,Yu.N,(1962),Sov.Phy,7,543.

14. Denisyuk,Yu.N,(1963),Optics and Spectroscopy,15,279.

15. Denisyuk,Yu.N,(1965),Optics and Spectroscopy,18,152.

16. Silverman B.A,Thompson B.J andWard J.H.(1964), J.Appl.Metrol,3,792

17. Thompson B.J,(1963),J.Soc.Photo.Opt.Inst.Eng,2,43.

18. Parrent G.B and Thompson B.J,(1964),Opt.Acta,11,183.

19. van Heerden P.J,(1963),Appl.Opts,2,387.

20. van Heerden P.J,(1963),Appl.Opts,2,393.

21. Vander Lugt A,(1964),IEEE Trans.Inf.Theory,10,139.

22. Stroke G.W, Resetrick R,Funkhouser A and Brumn D, (1965),Phy.Lett, 18,224.

23. Thompson B.J, Ward T.H and Zinky W.R,(1967), Appl.Opts., 6,519.

24. Kogelnink H,(1967), Bell System Technical Journal.,44,2451.

25. Leith E.N and Upatnieks J.(1966),J.Opt.Soc.Am,56,523.

26.Brooks R.E, Heflinger L.O and Wuerker R.F,(1965), Appl.Phy.Lett.,7,248.

27.Collier R.J, Doherty E.T and Pennington K.S,(1965), Appl.Phy.Lett.,7,223.

28.Hains K.A and Hildebrand B.P,(1965),Phy.Lett.,19,10.

29.Powell R.L and Stetuson K.A,(1965),J.Opt.Soc.Am.,55,1595.

30.Aleksandrov E.G and Bouch-Bruevich A.M,(1967), Sov. Phy-Tech.Phy,12,258.

31.Rogers G.L,(1952),Proc.Roy.Soc,63A,193.

32.Kock W.E,Rosen L and Rendeiro J,(1966),Proc.IEEE,54,1599.

33.Schwar M.J.R.Pandya T.P and Weinberg F.H,(1967),Nature, 215,239.

34.Benton S.A,(1969),J.Opt.Soc.Am,59,1545.

35.Chang B.J,(1973),Opt.Comm,9,357.

36.Cross L,(1977),Proc.SPIE Seminar on 3-D imaging.

37.HuignardJ.P,Herriau J.P,AubourgP and Spitz E,(1979), Opt.Lett,4,21.

38.Jordan,Jr,R.A,IBM J.Res.Dev.14,476.

39.Lee W.H,(1970),Appl.Opt.,9,639.

40.Lee W.H,(1974),Appl.Opt.,13,1677.

41.Hariharan P,Oreb B.F,and Brown N,(1983),Appl.Opt.,22,876.

CHAPTER II

EXPERIMENTAL SETUP, CO-ORDINATION AND OPTIMISATION

Abstract

Fabrication details and essential vibration characteristics of a low cost holographic table, in which the main vibration absorber is rubberised coir, is described. Methods of vacuum deposition of mirrors ,varying density beam splitters,the indigenous method used to make spatial filters and the design details of other mechanical components such as micropositionable plate holders and positioners are given. The elementary experiments done by using the setup are also presented.

BASIC EXPERIMENTAL SETUP, CO-ORDINATION AND OPTIMISATION

2.1 Vibration isolation table

2.1.1 Introduction

Since wavelength of visible light is too short, nearly half a micron , it may be impossible to conduct any interferometric experiment in the presence of vibrations. Also the surface on which an optical setup is mounted must satisfy some basic requirements. It must be stable , rigid and should remain isolated from ambient ground vibrations. It must also damp quickly the vibrations, if any,produced by any individual active component in the setup. But , considering the high cost of a pneumatically isolated table constructed with honeycomb core and the performance of metal spring isolators, inflated rubber tubes, ordinary concrete and granite structures, there arises the need for new design of optical tables giving an all round performance within the domain of the demands and investments of a research laboratory.

Ordinary steel springs cannot be used as isolators because of their poor damping and large static deflection [1]. The natural frequency of rubber [2] and the large value of supporting area to volume ratio prevents one from using inflated rubber tubes. But rubberised coir, a cushion material which consists of coiled coconut-husk fibers spray coated with

rubber, combines the good qualities of both rubber and spring. Because of the woody fibrous structure,it has spring-type behavior and also vibration absorbing capability [3] in lower frequencies.

2.1.2 Table design

Holographic work requires that if the table picks up vibrations the relative path length changes across the table surface should not exceed a quarter of a wave length, during exposure [4]. The present design is shown in Fig.2.1. The main part of the design is a heavy iron table (mild steel) with top dimensions 1.5 x 1 x 0.005 m^3. The table has six legs made of mild steel pipes of 0.05 m diameter and metal bushes,0.002 m thick,are attached to the bottom of the legs. In addition to rubberised coir sheets, which provides dynamic rigidity (resistance of the table top to induced time-varying forces), plywood, which is also a good vibration absorber [5] is used to ensure static rigidity (resistance of table top to static forces). The

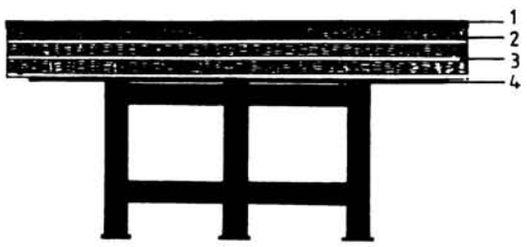

Fig.2.1 Front view of the table
1. Mild steel top-skin.
2. Rubberised coir layer
3. Ply-wood sheet
4. Mild steel plate forming the table top

thickness and number of plywood and rubberised coir sheets are adjusted to obtain an optimum performance. The height of the entire setup was 0.9 m, which conveniently served the purpose of a standard experimental table.

2.1.3 Experimental setup for vibration analysis

The three primary criteria for comparing table performance are the structural frequencies, damping and compliance values. The transmissibility, defined as the ratio of the amplitude of the transmitted vibration to that of the forcing vibration, for various frequencies and table top-skin weights were measured by using an electromagnetic vibration exciter and electromagnetic sensor (SYSCON) [6].

This vibration exciter consists of a powerful magnet, centrally surrounding which is suspended an exciter coil . If an alternating current is injected into the coil, the coil moves up and down continuously. By controlling the amount of coil current , the amplitude of vibration can be controlled. The system also consists of a tunable sine wave oscillator and a power amplifier. The vibration sensor is also electromagnetic type and consists of a permanent magnet and a coil suspended in magnetic field [7]. The system has been designed to have a very low resonant frequency. When the sensor is brought in the vicinity of any vibrating object, an emf is induced in the coil by the magnetic field,which is processed by the vibration indicator for the measurement of displacement, frequency or velocity of the vibration. The exciter and sensor both have a frequency response of 1Hz to 10 KHz. It has been possible to measure displacements of the range of 0.1 to 1000 microns. The

instrument has built in voltage regulators to accommodate ± 10% change in mains voltage.

2.1.4.Experimental results.

The transmissibility variation with frequency and table top skin-weights are given in Fig. 2.2. when the skin weight was 275 kg, almost all disturbances were attenuated except for frequencies near 21, 31 and 56 Hz, where the transmissibility was less than 15% This was reduced to 7% by placing the legs of the table in wooden boxes containing rubberised coir and sand.

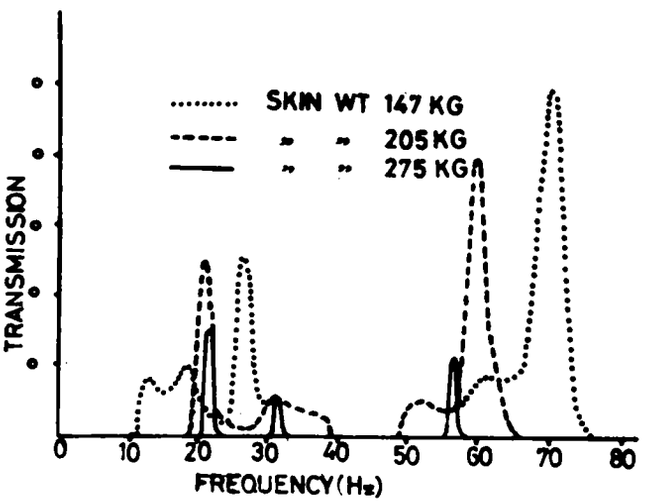

Fig.2.2 Transmissibility for differenet table top skin weights

The present design excludes the ground frequencies usually picked up by tables,which are in the frequency range of 2-4 Hz.An attempt was made to assess the vibration isolation by using a Michelson interferometer type setup and the electromagnetic vibration exciter.It was found that the jitter of the interference fringe pattern observed at 21, 31 and 56 Hz decreased as the loading increased and vanished at a load of 310 kg.

Damping rate on the table top corner was measured using a Tektronix storage oscilloscope and was found to be 68.54 dB S^{-1}.Typical tables claim hundreds of dB S^{-1}.The table

top damping for a table resonance frequency 21 Hz is given in Fig.2.3.

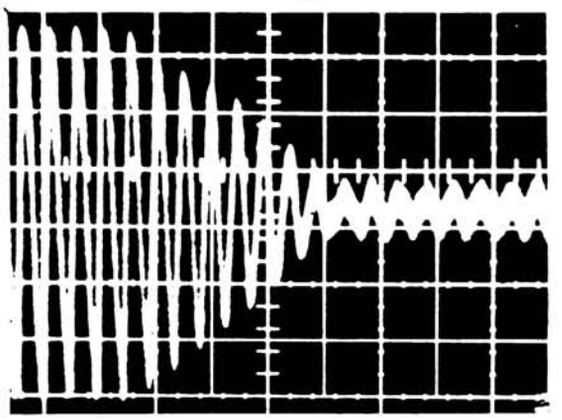

Fig.2.3 Table top damping at a table resonant frequency 21 Hz

Time - 0.2 sec/div

In the case of a static force, compliance is defined as the ratio of the displacement of a specific part of the table to the magnitude of the applied force.But for a dynamically varying force,it is the ratio of the excited vibrational amplitude to the magnitude of the forcing vibration.It is explicit that a table whose compliance is small is a good optical table.Low compliance value can be obtained by optimising damping,stiffness and mass.The compliance values on the table top corner for different sinusoidal forces,applied in the vertical direction (which is the case of practical interest are presented in Fig.2.4. From commercial data available this was found to be comparable to ordinary honeycomb structures without internal damping, better than that of concrete slab or

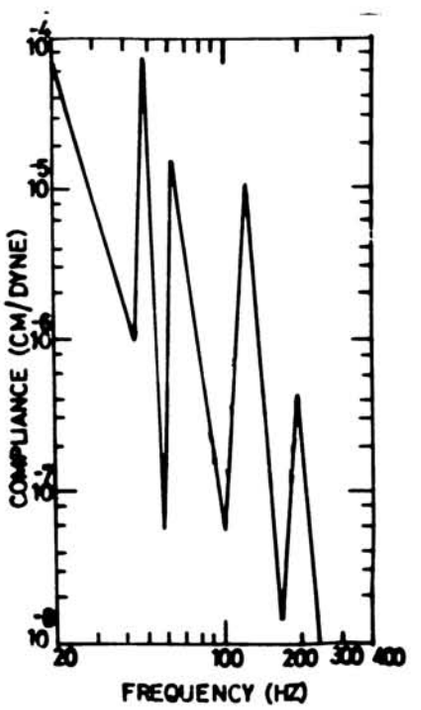

Fig.2.4 Compliance curve of the table top

steel plate and poorer than that of honeycomb structures with internal damping.

The present design costs Rs 10,000 which is about half the price of some of the cheapest commercial models with honeycomb structures and without internal damping.Good reconstructions of the holograms recorded at different environmental conditions implied the isolation capability of the table. The clarity and contrast of the photomicrograph of a hologram Fig.2.5 taken on the table, when a rotary pump was working in the room, compare favorably with similar micrographs of standard holograms [8]. The overall performance of this new design indicates that this low-cost design can be used for the satisfactory recording of holograms.

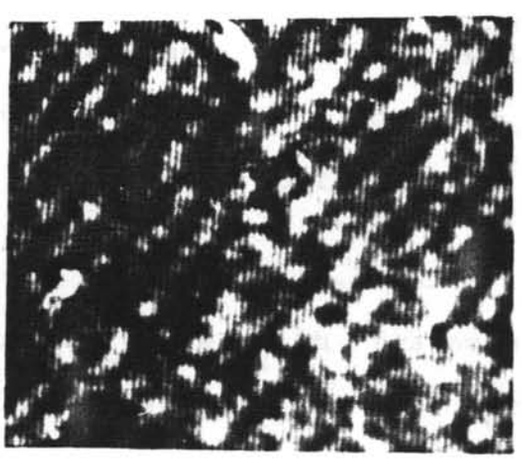

Fig.2.5 Photomicrograph of the Hologram

2.2 Optical and mechanical components.

In a basic holographic setup the laser beam has to be divided in to two or more component beams and each of this components has to be expanded to illuminate the object.For many experiments this expanded beam should be uncluttered and needs filtering. Thus a practical setup requires good quality optical components like beam splitters, beam expanders, beam filters

and beam directors. There should also be stable mechanical holders and positioners to hold the optical elements of different shapes and sizes. These should allow the required degrees of freedom of movements and adjustments.

2.2.1 Beam directors and beam splitters

For recording the hologram of any object, the object has to be illuminated uniformly. Similarly at hologram plane the reference beam also should possess uniform intensity. If an ordinary mirror is used to direct the laser beam the uniform intensity of the beam will be lost. This is due to the interference of beams reflected by front surface and back inner surface of the mirror.

Blanks cut from 10mm thick glass with flatness of about $\lambda/4$ has been used as substrates for making the mirrors and beam splitters. These glass substrates are thoroughly cleaned by different processes. Initially the substrates are cleaned by using soap solution and then dipped in freshly prepared chromic acid for a few hours to remove alkaline and other oxidising impurities [9]. The oxidation can be enhanced by warming the acid to 70^{0}C. The substrates are then washed in distilled water and transferred into an ultrasonic cleaner. The microscopic impurities are stripped off by the ultrasonic agitation [9,10] and the process is continued for about 20 minutes. After this the substrates are again cleaned in distilled water, dried slowly in a clean oven and transferred to a vacuum coating unit.

Vacuum coating unit

Mirrors and beam splitters are prepared by using thermal evaporation under high vacuum [9,11,12]. Schematic diagram of the vacuum coating unit for this purpose is given in Fig.2.6. The vacuum coating unit consists of a mild steel

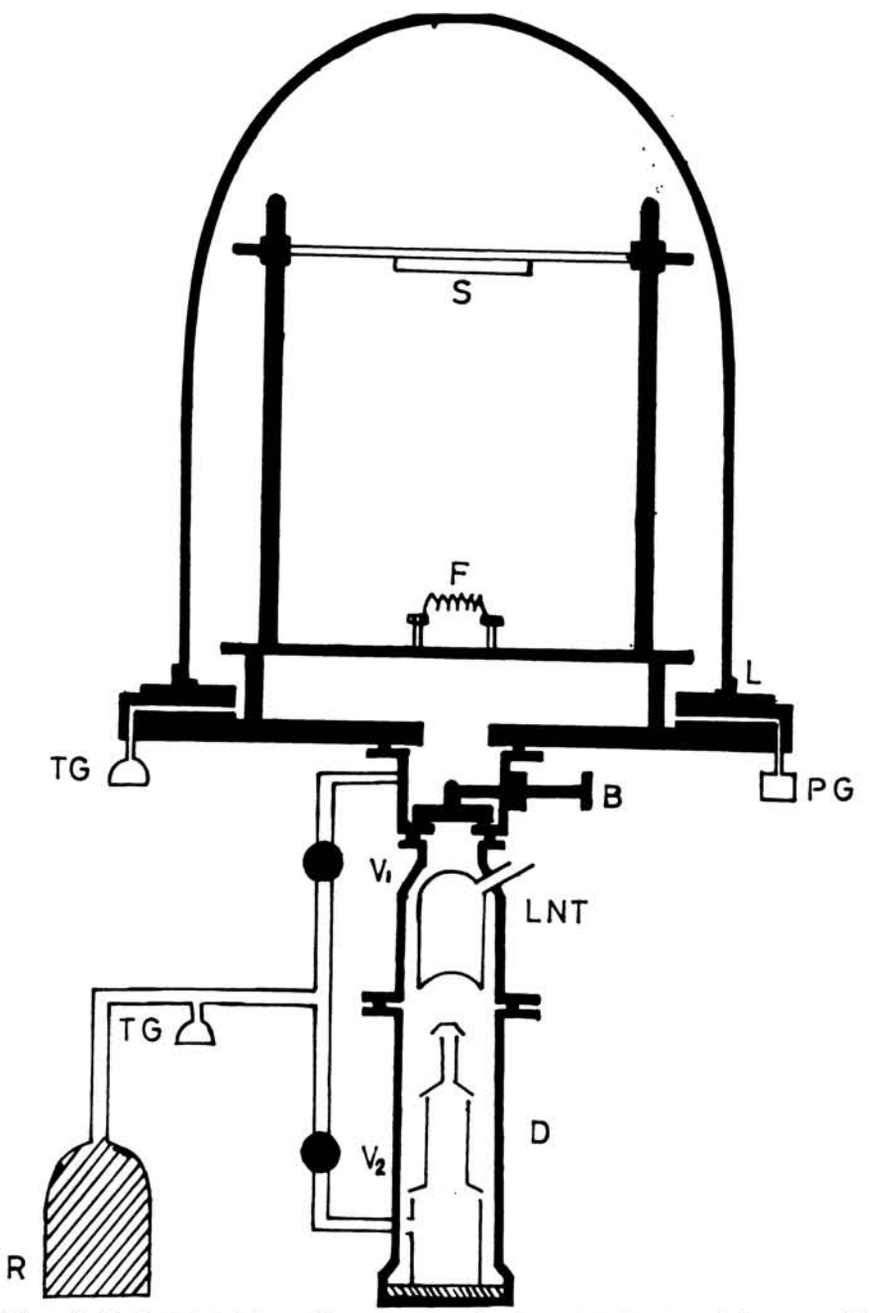

Fig.2.6 Scematic diagram of a vacuum coating unit

D - Diffusion pump , LNT - Liquid Nitrogen Trap,
B - Baffle valve, PG - Penning Guage,
L - Gasket S - Substrate,
F - Filament , TG - Thermocouple Guage,
R - Rotary pump, V1 - Diaphram valve for roughing ,
V2- Diaphram valve for backing.

base-plate, 550 liter/minute rotary pump and a 15 cm diffusion pump.The base-plate is chromium plated and has a bore of 19.5cm diameter at the center for connecting the diffusion pump. There are ports for fourteen feedthroughs, from the sides of the base-plates. Penning gauge and air admittance valve are connected using two of the side ports. Some of the other side ports are used for connecting high voltage and high current feedthroughs , thermocouples and substrates heater. There are two filament evaporators, so that they could be heated one after the other. Ports not in use are closed by dummies.A 30 cm glass dome is pressure-sealed on the base-plate using an L-gasket.

The diffusion pump is fitted to the base-plate through a baffle valve. The rotary pump (Toshniwal Bros.) is connected in series with the diffusion pump.It can also be used for roughing the whole system to 10^{-2}Torr. V_1 and V_2 are diaphram valves for roughing and backing the coating unit, respectively. 200 cc of silicon oil (DC 704) is used to charge the diffusion pump. A pressure of 10^{-5} Torr can be obtained in the dome. Filament holders and substrate holder are mounted on the base-plate.A high current transformer (100 Amp, 10 V)is connected to the filament holder. A high tension transformer is also provided for ion-beam cleaning.

During deposition of mirrors the substrates are mounted horizontally at 20 cm above the filament. Tungsten spiral or molybdenum boats are used as heating elements. After loading the cleaned substrates, before the deposition of the

film, ion-beam cleaning system has been activated for about 20 minutes to remove microscopic contaminants and oxides from the substrates [9,10].

Aluminium is the most widely used material for reflecting metal films. It has consistently high reflectance throughout the visible and near IR regions [13] of the spectrum. Silver gives slightly higher reflectance compared to aluminium through most of the visible region , but it has the disadvantage that it will be tarnished quickly due to oxidation, compared to aluminium. The exposed surface of aluminium also oxidizes, but slowly, and this oxide acts as a very thin tough and corrosion resistant layer.

Protected aluminium and silver are two best practical general purpose metallic coatings in the visible and near-infrared region. Protected coating is a coating covered with a dielectric film of magnesium fluride (MgF_2) or silicon monoxide (SiO) of about $\lambda/8$ or less optical thickness. This protective film prevents oxidation and helps to preserve the initial high reflectance.

Films are made by evaporating the metal by using the tungsten spiral or molybdenum boat, depending upon the nature of the substance. The metal is evaporated at a pressure of about 10^{-5} Torr. In the case of mirrors, substrate heating during coating could not be done due to tarnishing of the film even before the deposition of the protective coating. Usually metal is kept in one of the heater elements and the dielectric in the other. Silver films can also be protected by giving a

very thin over coating of copper. In the case of silver films it was particularly noted that the edges of the films have to be covered by the dielectric layer because there are chances of spot formation on the film due to absorption of moisture. Good quality mirrors could be deposited and the substrates where of $5 \times 5 \times 1\ cm^3$ and $10 \times 10 \times 1cm^3$ dimensions. Percentage of reflectivity and the variation of reflectivity with wavelength of the mirrors with and without protective coatings are given in Fig.2.7a and b. The thickness of the films were of about $2000^{\circ}A$.

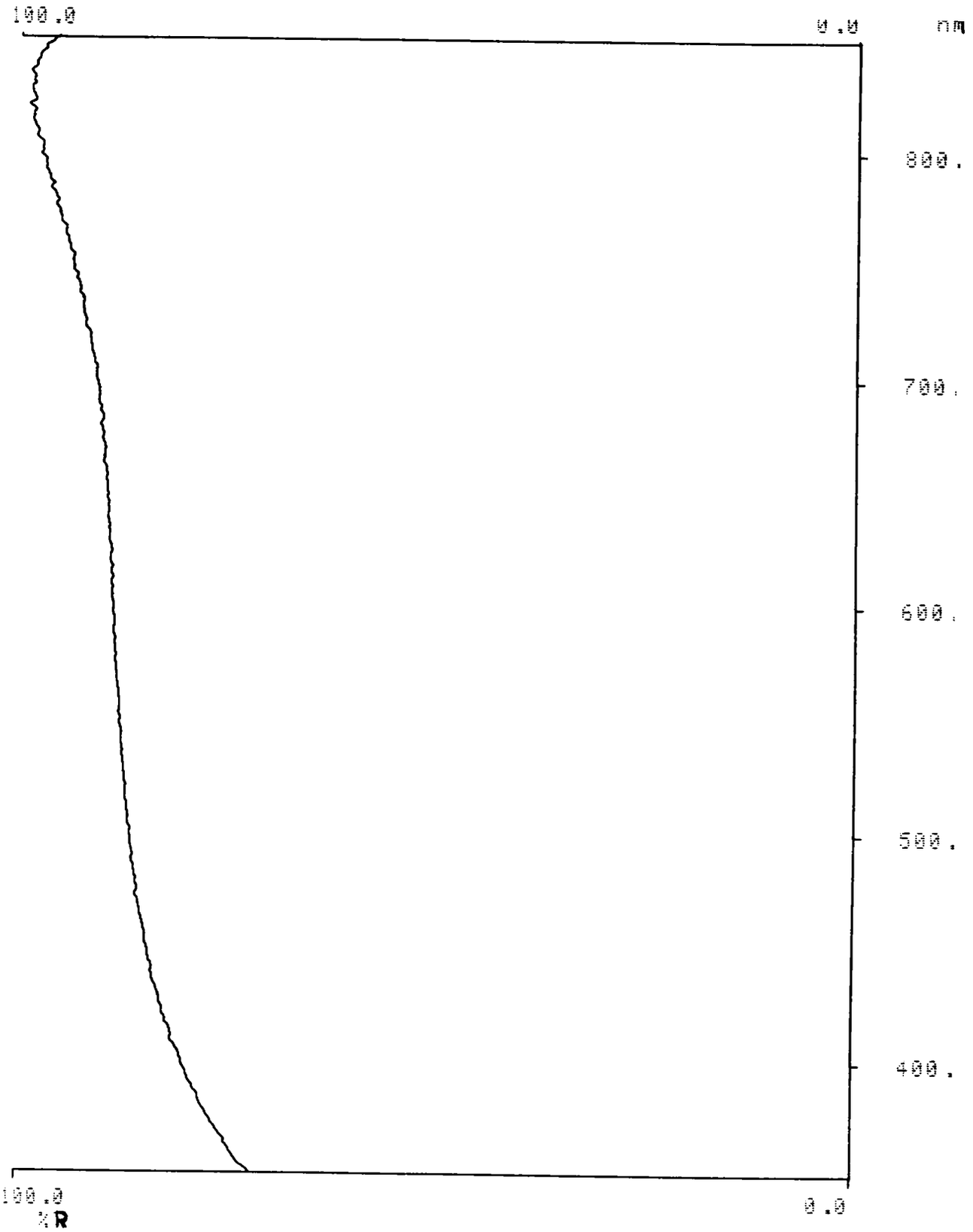

TITLE: AL MIRROR SPEC REF 12:55 AM 7/ 1/90
SCAN SPEED: 120 (240) nm/min RESPONSE: MEDIUM
BANDPASS: 2.00nm/SERVO GAIN=1

Fig.2.7a Reflectivity variation of the aluminium mirror compared to a standard aluminium mirror of reflectivty 86%.

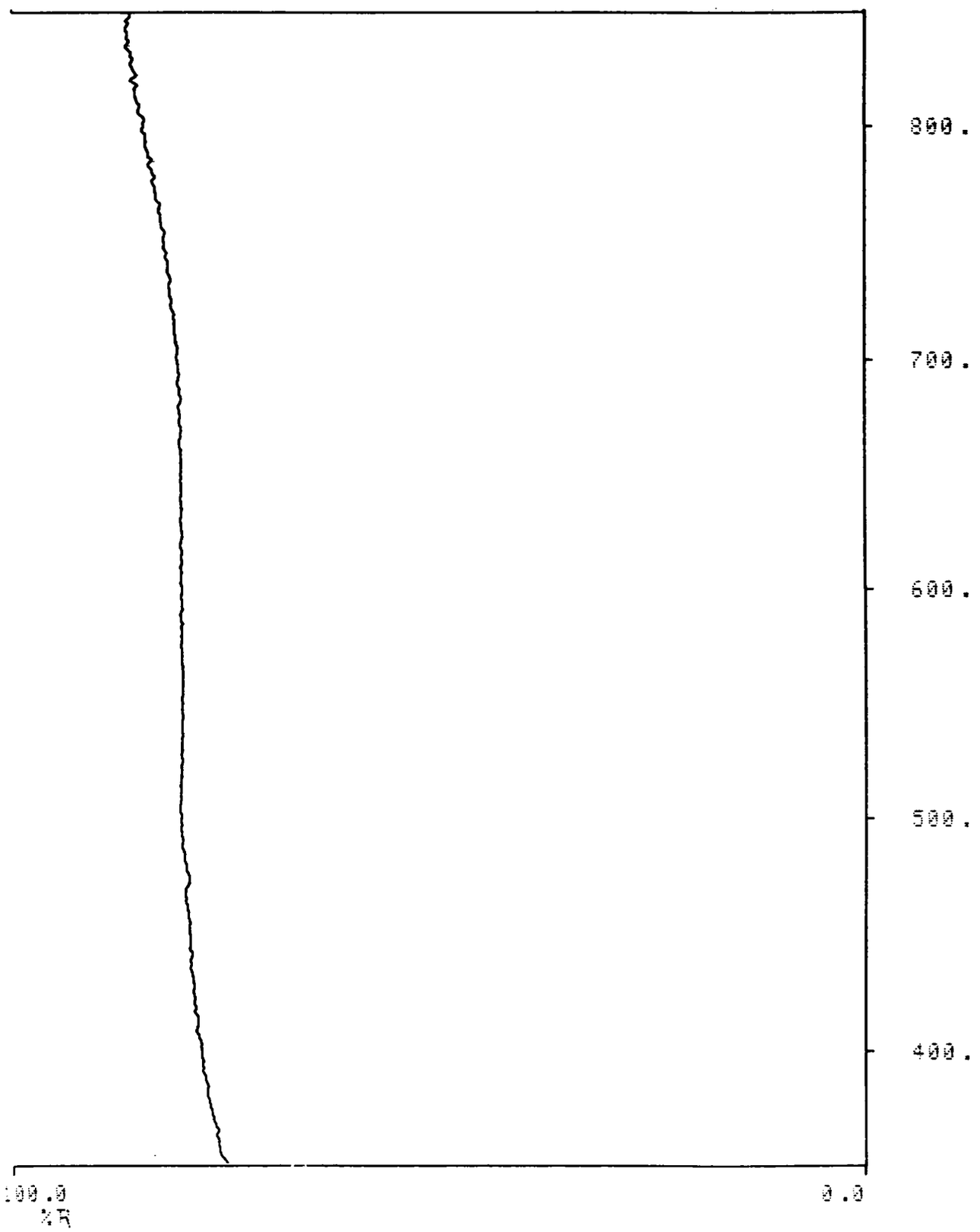

TITLE: AL MIRROR SPEC REF 11:50 PM 6/30/90
SCAN SPEED: 60 (120) nm/min RESPONSE: MEDIUM
SLITPASS: 2.00nm/SERVO GAIN=1

Fig.2.7b Reflectivity variation of the aluminium mirror with λ/8 thick protective MgF_2 coating.

Beam splitters are also coated(Al and Ag films) by using the above procedure .The transmittance or reflectance of the film can be controlled by varying the thickness of the film. A thickness monitor, fabricated [14] in the Department was used for this purpose. In this monitor a chopped beam of light, after reflection from the sample,is allowed to fall on a photo diode. A tuned amplifier amplifies the signal from the photo diode and the output is read on a meter or chart recorder.Different filters are also provided for wavelength selection.

During experiments plate-beam splitters have to be changed in order to adjust the beams-ratio and hence beam splitters with different reflectivities have to be coated. This inconvenience can be avoided by using a varying density beam splitter. A special technique has been used to prepare beam splitters with varying reflectivity.In this method the substrates are mounted vertically at a particular height from the filament. Assuming a point source, the thickness of the film on a substrate point situated at a distance r from the source is [15] given by

$$t = \frac{m}{4 \pi \rho r^2} \qquad (2.1)$$

where m - mass of the substance evaporated and

ρ - its density.

If we use a long substrate which is vertically mounted in the dome, different heights on the substrate will have different film thickness. Beam splitters with different reflectivities and reflectivity variation are deposited by

varying the height of mounting and the angle between the substrate plane and the horizontal, respectively.

Three beam splitters on 12 × 1.5 × 1 cm^3 glass substrates were prepared for three angles of holding. One substrate was held vertically and the others in 20^0 and 40^0inclination with the vertical, at a distance 14.5 cm from the source.The aluminium films were deposited on the substrate so as to have a film thickness of about 400^0A at the bottom.The transmissibility variations of these beam splitters (Fig.2.8 a, b and c), with distance are measured by using a spectrophotometer (Hitachi-U3410).

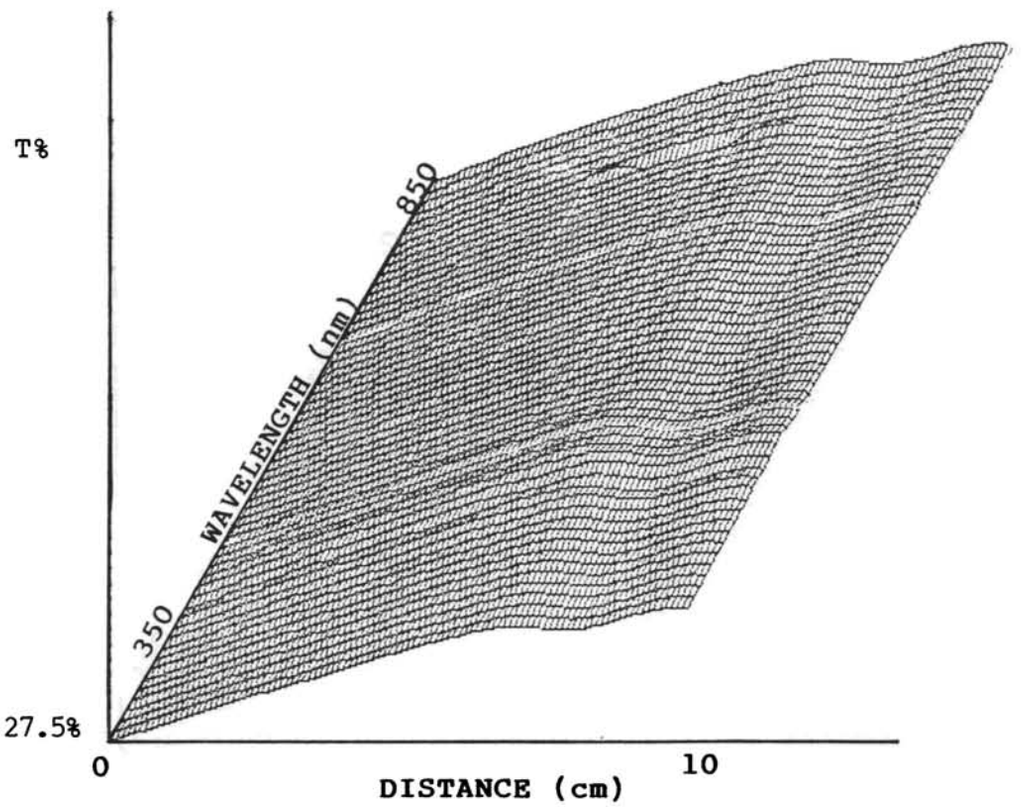

Fig.2.8 Transmissibilty variation of the beam splitter

a. Vertically held.

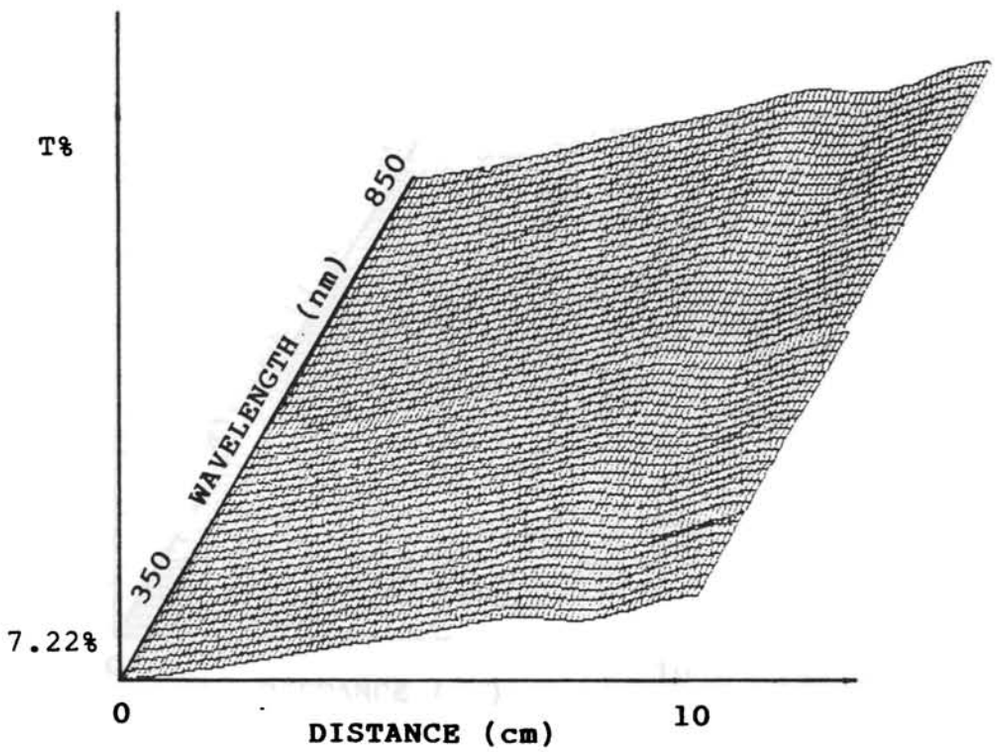

Fig.2.8 Transmissibilty variation of the beam splitter b. -20^{o} with the vertical.

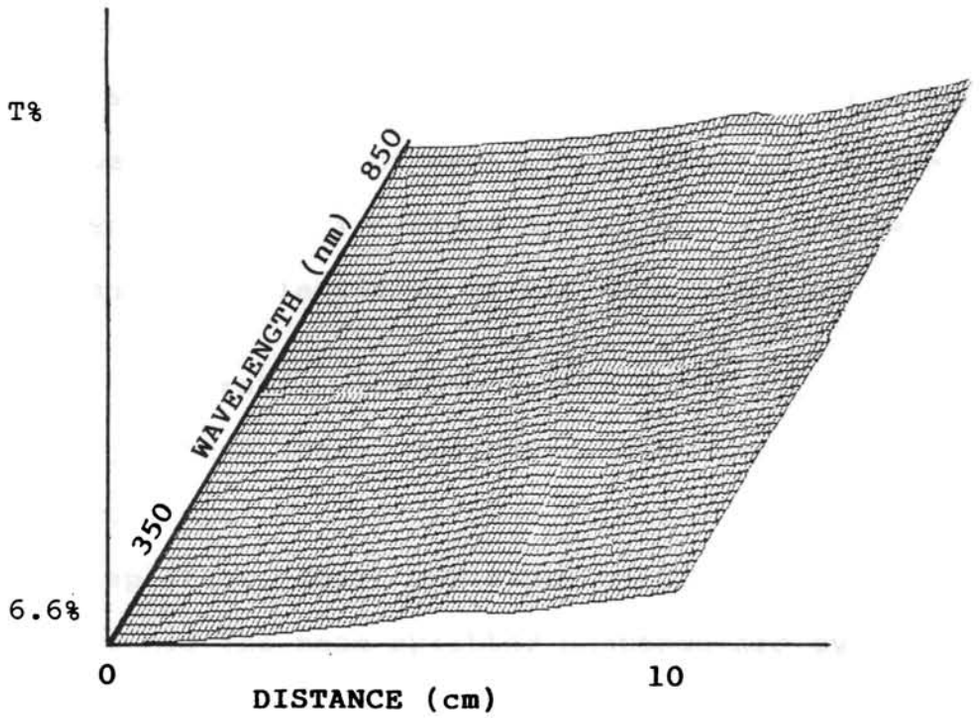

Fig.2.8 Transmissibilty variation of the beam splitter

c. -40° with the vertical

Beam splitters of about 50% maximum reflectivity can be ingeniously deposited with the help of a standard semitransparent film. For this the bottom of the beam splitter substrate has to be mounted at a distance from the filament which is same as the distance of a particular point on the dome, from the filament.During evaporation keep the semitransparent film at this point outside the dome and looking through it deposit the film until the view of the filament disappears.If standard coatings with different reflectivities are available on thin substrates this technique can be used to prepare beam splitters of desired reflectivities. The accuracy of the method can be increased by having a knowledge of the absorption and reflectivity at the dome surface.

Substrates with dimensions 4 × 4 × 1 cm^3 are used for making these beam splitters.Thick substrate helped to separate the spurious reflection from the inner back surface of the beam splitter, which may cause problems during the spatial filtering. All the beam splitter coatings are over coated with protective coatings to enhance the life. Single layer MgF_2 anti-reflection coatings are also tried with the help of the thickness monitor.These coatings are applied on the back side of a few beam splitters and the spurious reflection has been considerably reduced by this. All these optical surfaces are kept shielded from dust and other contaminants such as oil and fingerprints. However,in practice it becomes necessary to clean the surface and good care is required to avoid scratch and dig while cleaning. Clean and dry pressurised gas can be used for blowing off the dust. Metal coatings and other soft coatings can be cleaned with a quick and gentle flush with electronic

grade acetone. Protected metal coatings can be cleaned best by using a clean sheet of lens tissue. Put a few drops of acetone on the center of the tissue and pull it across the mirror. The dry parts of the tissue helps to remove the acetone residue.Repeat this until the mirror is cleaned. Use a new tissue for each wipe.

All the optical components were covered with polyethylene bags and it could be possible to use same mirrors and beam splitters for several months.

Thickness measurement

An idea about the thickness of the film can be obtained from the mass of the material evaporated. Assuming a point filament source, the thickness of the film on substrate situated far away from the source is given by the equation 2.1. For strip source the thickness will be twice the above value [15]. In practice these sources are not point sources and hence the thickness calculated is only approximate. (Mass of the material is measured accurately by using an analytic micro balance) . Wherever more accuracy is needed, the thickness is measured by using the optical interference method [16]. Here a partially reflecting surface is kept on a totally reflecting surface to form an air-wedge and interference fringes are produced by a monochromatic parallel beam with wavelength λ. The shift of the fringes over the film step edge and the fringe separation can be measured by using a travelling microscope. Thickness of the film is then given by

$$\frac{\lambda \times \text{fringe shift}}{2 \times \text{fringe separation}}$$

The experimental setup used for this measurements is the same as that presented in [16].

2.2.2 Spatial filters

A laser beam must have a smooth intensity profile for its many uses in holography and optical data processing. But, in practice the beam picks up undesirable intensity variations effected by the interference from light scattered by dust particles on the lenses and mirrors, and from lens defects. This results in fluctuations in the ideal TEMoo intensity profile of the beam Fig. 2.9a.This problem of `noise' can be tackled with the help of a lens-pin hole arrangement.Focusing the noisy beam forms the optical power spectrum of the distribution at the focal plane of the converging lens.At the focal point the pin-hole acts as a low pass filter Fig.2.9b, by passing only the undisturbed portion of the laser beam.

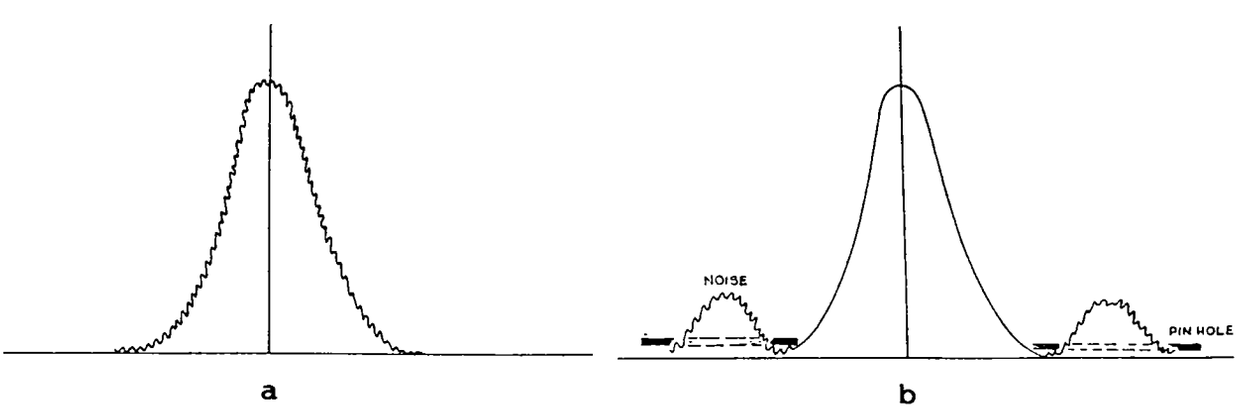

Fig 2.9 A representation of spatial filtering.

a. Unfiltered beam.

b. Filtered beam.

The instrument consists of a short focal length converging lens movable along the x and y axes and a pin-hole movable along the z axis. The power of the lens determines the divergence of the expanded beam and the pin-hole aperture controls the degree of filtering.In the spatial filter fabricated we have used commercially available microscope objectives of power 10X and 20X. Pin-holes whose aperture range from about 50 to 20 microns are made in the laboratory.

Thin aluminium sheets on photographic packing paper are used for this.At first small circular sheets with diameter 1.5 cm are cut from these sheets and the aluminum foils are peeled off by putting in liquid detergent solution for a few hours. These thin wafers are then cleaned thoroughly and dried. A very fine tipped needle, selected from a set of needles with the help of a microscope is then used to drill the wafer. The wafer is placed on a soft surface and drilled carefully with the needle.On the other side of the drilled wafer there forms a small projection. If we keep this drilled wafer in between two cleaned glass plates and press, we can reduce the diameter of the pin-hole.The pin-holes are then cleaned using ultrasonic cleaning technique. The aperture of the pin-holes are then tested and measured by using a comparator. To cite a typical example, a pin-hole with initial diameter of 260 microns was reduced to 90 microns after pressing in between the glass plates.

Photographs of the spatial filter arrangement (Fig2.10) and that of the unfiltered and filtered beams, at a distance of 25 cm from the lens are given in Fig. 2.11a and 2.11b. Unwanted play in the x-y-z translator is arrested by using a gib and screw arrangement.

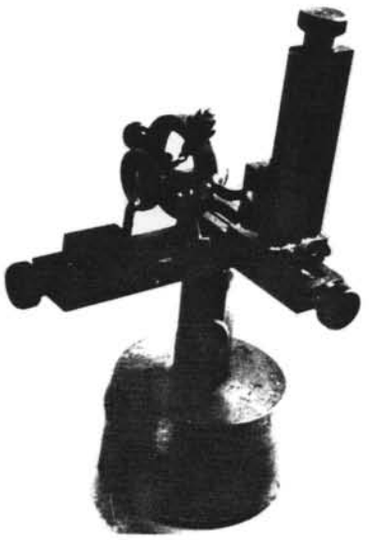

Fig 2.10 Fabricated spatial filter.

2.11a 2.11b

Fig 2.11 Expanded laser baem at distance of 25 cm from the lens.

a. Before filtering. b. After filtering.

2.2.3 Holders, Positioners and other system components.

A range of holders and positioners are designed and fabricated so as to satisfy the general and some special needs of holographic experiments. Special care has been taken for allowing the necessary degrees of freedom of movements and adjustments.Laser holder with fine adjustments, adjustable mirror and beam splitter mounts, adjustable-radius chucks, holders for collimators, multipurpose holders for beam steering, plate holder and micropositionable plate holder come in this set Fig.2.12.

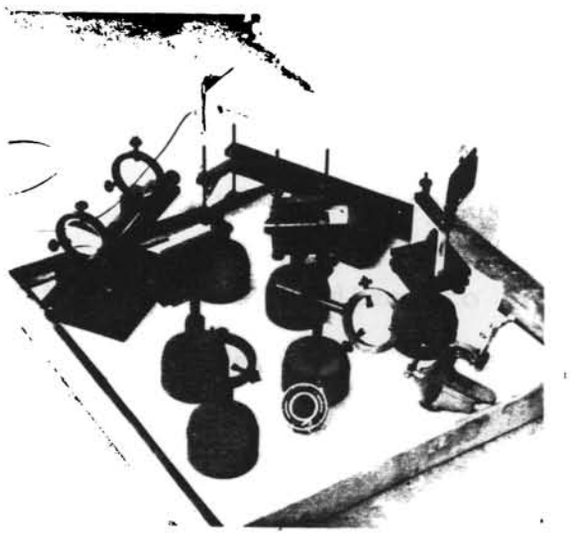

Fig 2.12 Holders and positioners.

Micropositionable plate holder has been used for recording some real-time holograms. This holder mainly consists of two parts. The bottom part which is fixed to a magnetic base has three steel balls Fig.2.13, welded on a mild steel slab; so as to form a triangle. The size and position of the balls are such that it exactly fits in a `T' shaped wedge on the top part , which is

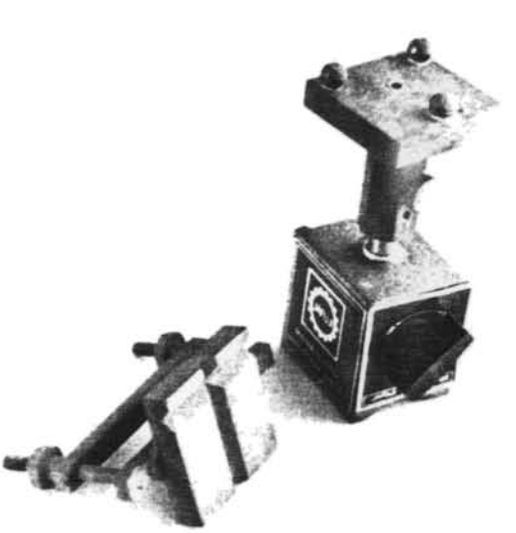

Fig.2.13 Micropositionable plate holder.

the movable part.There are arrangements in the top part for holding holographic plates tightly. Movements in the horizontal plane are arrested by the wedge-ball arrangement and helps the exact repositioning of the developed plate.Care should be taken against dust and rust particles at the points of contact.

All the holders and positioners are anodized to avoid unwanted reflections and to ensure long life.

A mechanical shutter equipped with `T' and `B' settings and having a maximum speed of 150^{th} of a second has been used for the exposure control.

2.3 Elementary experiments on Holography

The initial setup used for recording holograms is shown in Fig.2.14. A 10X microscope objective along with a 30 micron pin-hole is used in the setup for spatial filtering. A

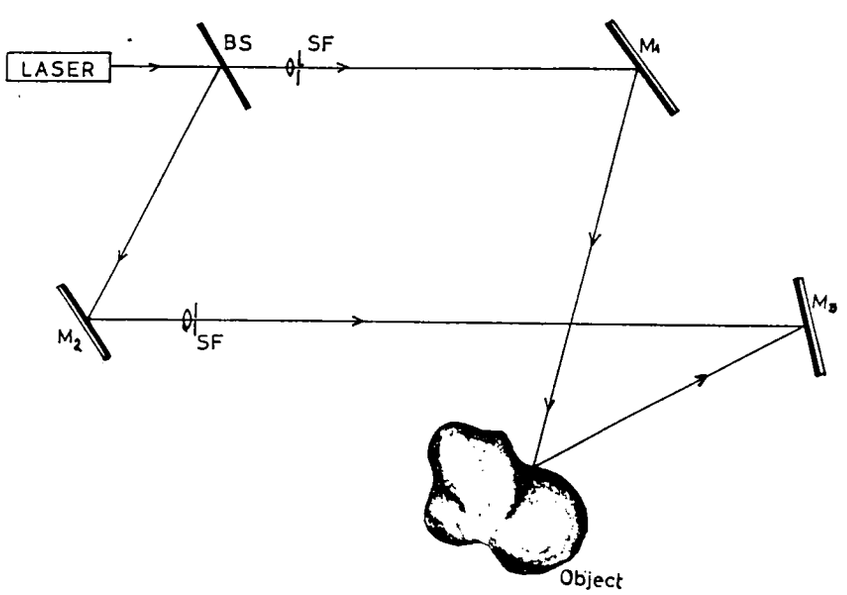

Fig 2.14 Initail holographic setup used.

10 mw He-Ne laser beam was allowed to pass through the center of the lens. The lens-pin-hole spacing was then adjusted so as to locate the pin-hole at the focal plane of the lens. The adjustments in the vertical and lateral directions were made to locate the pin-hole at the focal point. A sheet of white paper was placed in front of the spatial filter to collect the spot of light. If this bright spot was surrounded by rings, then the focusing was slightly adjusted by moving the pin-hole. Finally fine adjustments on the lens adjusting screws were done to obtain an optimum brightness and roundness for the spot.

The path length of the reference and object beams were made almost equal and the beam splitter was adjusted to set the beam-balance ratio. A laser power meter (EG & G-Gamma Scientific, Model 460-1A) was used for this. Initially the reference beam intensity at the hologram plane was made about six times stronger than that of the object beam. The path length and the angle between the beams were set to 200 cm and 40° respectively. Agfa Gevaert 10E 75 Holographic plates of 3 x 2.5 cm^2 were used for recording the holograms.

The optimum exposure time of 2 sec. was found by trial and error method. The developer used was four times diluted Agfa Gevaert-A903 universal developer. Development was carried out for about 5 minutes at $24^{\circ}C$, followed by a short rinse in distilled water and three minutes fixing in Agfa Gevaert rapid fixer. Processed plates were washed in running water for about 8 minutes.

The angle between the interfering beams and the distance of the object from the hologram plate were varied and

holograms of objects with different sizes were recorded. Good reconstruction of the holograms (Fig 2.15a - e),implied the

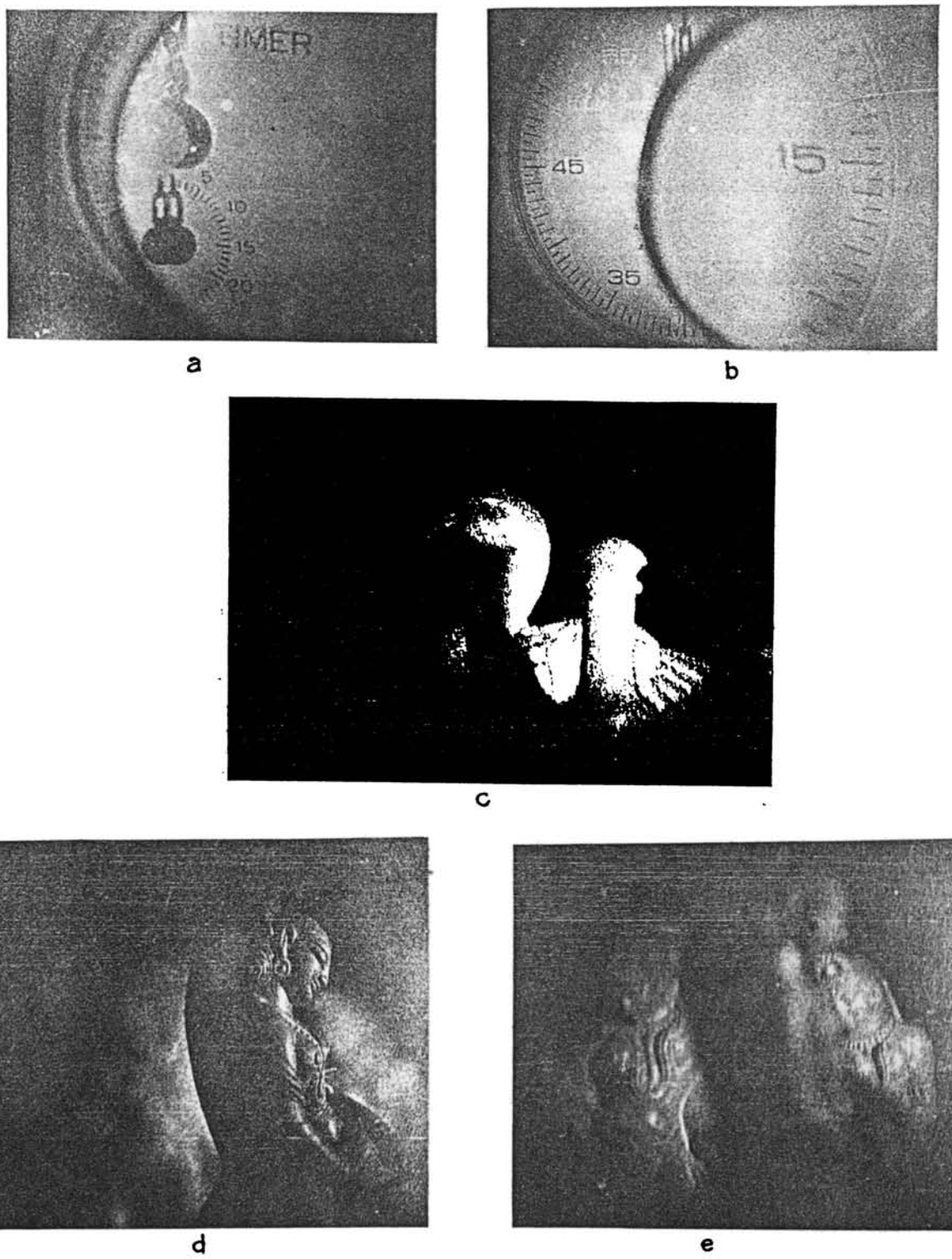

Fig.2.15 Different perceptions of a few simple holographic reconstructed images
a,b. Horizon tal parallax in a watch and lens arrange ment.
c. Swan and a pawn
d,e Camera focused on different points of an image to show the depth of field.

freedom of the setup from vibrations and the quality of the optical and mechanical components used in the setup. Some of the over exposed holograms (absorption) were bleached by using 5% aqueous solution of potassium ferricyanide [18] and were converted into phase holograms. In all these cases the brightness of the reconstructed images were found to be enhanced.

Young's modulus of an aluminium plate (6 × 2 × 0.15cm^3) was calculated by using the combined application of cantilever principle and double exposure holography. The aluminium plate was fixed vertically and small weights were added in a pan and pulley arrangement attached at the free end of the plate. First exposure was made with a dead load and the second with four grams added to the pan. Fourteen fringes were observed in the reconstructed image. The displacement for this particular load was calculated from the fringe number n, viz.,$n\lambda/2$ and the Young's modulus was calculated. The experimental value 71.46 × 10^{10} agreed well with the reported [19] value 68.9 × 10^{10}dynes/cm^2.

Time averaged holograms of a vibrating loud speaker, excited at a particular frequency, with the help of an AF signal generator, was recorded. The amplitude of vibration was adjusted so as to yield a clear reconstruction. The reconstructed image of the diaphram consisted of fringes as given in figure 2.16.

Fig.2.16 Reconstructed image of a vibrating loud speaker.

References

1. Macinate,"Seismic mountings for vibration isolation", John Wiley and Sons,New York,(1984),Chap.5, p 110.
2. Edward Miller (Ed),"Plastics products design Handbook",Part A, Dave.S, Steinbrg, Marcel Dekker. Inc. , New York, (1981), Chap 11, p 410.
3. Ajith Kumar.P.T, Nair.E.M.S and Purushothaman, C. J. Phys.E.. Sci. Instrum. 19,643,(1986).
4. Vest.C.M,"Holographic interferomery", John Wiley and Sons New York,(1979).
5. Porter.A.G and George.S."Am J. Phys", 43,954,(1975).
6. Collacott.R.A,"Vibration monitoring and diagnosis",Wiley, New York,(1979), Chap.7,p 129.
7. Operation Manuél, Syscon Vibration Indicator.
8. Ostorovsky.Yu.I,"Holography and its Applications",Mir , Moscow, (1973), p 39.
9. Maissel.L.I and Glang.R (Eds.),"Hand Book of Thin film Technology", Mc Graw-Hill, (1970), p 6-39.
10. Chopra.K.L, "Thin film phenomena", Mc Graw-Hill, New York, (1969), p 62.
11. Holland..L, "Vacuum deposition of thin films", Chapnanand Hill, New Fetter lane, London (1970).
12. Roth.A, "Vacuum Technology", North Holland Publishing Co., Amsterdam, New York (1976), Chap 7, p 329.
13. Walter.G.D, William Vaughan, "Handbook of Optics (Opt.Soc.Am.), Magraw Hill Book Co., New York, 1978.
14. Project report, Ambadi, Dept. of Physics, CUSAT,(1986).

15. Robert W.Berry, Peter M.Hall and Murray T.Harris, "Thin Film Technology, Van Nostraud Rheinhold, New York, p.160 (1960).

16. Chopra.K.L,"Thin film phenomena", Mc Graw-Hill,(1969), Chap. 3, p.102.

17. Maissel, L.I and Glang, R, "Handbook of Thin film Technology",. Mc Gaw-Hill, New York Chap.11, p.7.

18. Collier R.J, Burechardt, C.B and Lin, L.H."Optical Holography", Academic Press, New York (1971), p.291.

19. American Institute of Physics Handbook, (3rd Edn), Mc Graw Hill (1972) p.2.63.

CHAPTER III

STRESS MEASUREMENTS IN THIN FILMS BY USING HOLOGRAPHIC INTERFEROMERTY

Abstract

Stress in thin films is attracting growing attention because of its problematic role in many applications.There are different techniques for measuring the deflections produced by stress in thin films, such as bending beam-method ,disc method, x-ray and electron diffraction methods. We have made an attempt to observe the variation of thermal stress in different thin films, by using real time holographic interferometry. In the case of reflecting thin films we could observe real fringes both in the reference as well as in the object beam directions. These fringes were of very good visibility compared to common real-time holographic fringes and can be conveniently used for the measurement of stress in reflecting thin films.

STRESS MEASUREMENTS IN THIN FILMS BY USING HOLOGRAPHIC INTERFEROMETRY

3.1 Introduction.

3.1.1 Holographic interferometry.

Holographic interferometry is the interferometric comparison of two or more waves, at least one of them being reconstructed by a hologram. A hologram permits storing of a wave front and that can be compared to any wave front which is separated in time or space [1]. Holographic interferometry has got three main branches ie. two exposure holographic interferometry, real time holographic interferometry and time averaged holographic interferometry. The development of two exposure and real time holographic interferometry occurred independently in several laboratories in 1965 [2-8].

In two exposure holographic interferometry interference takes place between the wave fronts reconstructed by two holograms of the object exposed on the same photographic plate. If the wave front from an object is stored holographically and later compared to that coming from the object at different times, then it is real time holography. The third branch ie. time averaged holography will be discussed in Chapter IV.

Applications of holographic interferometry and related techniques fall into metrology, nondestructive testing, contour generation, flow visualization and measurement, solid mechanics and biomedical instrumentation. In all the above applications the primary quantity displayed by and determined from holographic interferograms is a change of optical path length. This change of optical path length, which is related to some physical property of interest may vary wildly in the above application areas.

3.1.2 Stress in thin films

The literature concerning the mechanical properties of thin films is not as extensive as that of the electrical and magnetic properties. Reliability of any thin film device depends to a large extent on the mechanical stability which in turn depends on the adhesion of the film to the substrate and the internal stress developed during deposition.Almost all thin films, irrespective of the means by which they are produced are in a state of internal stress. Existence of large stress has been known since the work of Stoney [9] on electro plated films.

Stress may be compressive or tensile depending upon the direction of expansion of the film. In the first case the film would try to expand parallel to the surface and in the second case it would try to contract. The total stress (Fig.3.1)in thin films consists of two major components,

Fig 3.1 Film-substrate composite under stress

`intrinsic' stress and `thermal' stress. Intrinsic stress results from incomplete structural-ordering [10] in the film arising during the growth and due to film contamination. The latter component results from the different thermal expansion coefficients of film and substrate. If the deposition temperature differs from the temperature during the measurements, depending upon the differential thermal expansion there is a compressive or tensile stress.

Thermal stress in thin films is attracting growing attention because of its problematic role in applications of thin films, such as masks and devices in micro electronics [11], thin film solar cells [12] and thin coated elements in high power lasers and related optics. Stress developed in quartz crystal employed in thin film thickness monitors, due to successive coatings of different materials causes problems in high precision thickness measurements. In cryogenic films thermal stress affects the critical temperature of superconductivity [13-15]. Moreover mechanically stable coatings are required for most industrial applications.The thermal stress caused by the differential thermal expansion can

be sufficient to bend or break either the film or the substrate. The laser damage of thin optical films has become a topic in itself [16].

There are different techniques for measuring the deflections produced by stress in thin films, such as bending beam method [17-19] and disc method[20]. X-ray[21] and electron diffraction [22] methods are also used to deduce the stress from the measurement of lattice parameter change.

3.2 Application of holography in measurement of thin film stress.

As we have seen already, holographic interferometry is a very sensitive tool for metrology and nondestructive testing. Magill and Young [23] have reported on the use of double exposure holographic interferometry in the study of stress in evaporated thin films. The stress was studied by etching away the film and hence was not a nondestructive method. Ramprasad and Radha [24,25] had reported on a simple nondestructive method by using real time holographic interferometry, for the measurement of stress in thin films during evaporation and for testing the adhesion.

We have made an attempt to observe the variation of stress with temperature, in thin films, by using real time holographic interferometry. Initially thin films of cadmium sulphide on glass substrates were used as the object. These films were diffusely reflecting. Solution flow method has been used for the *in-situ* processing of the hologram. The film substrate composite has been considered as a beam freely supported at both ends.

3.2.1 Real time holography.

As discussed in Chapter I when the interference pattern of an object wave, with a reference wave is properly recorded and re-illuminated,a wave whose complex amplitude is linearly proportional to that of the original object wave can be reconstructed. If one can replace the processed hologram plate exactly in its original position, the reconstructed image of the object will be exactly superposed on the object; assuming that the object stays fixed in position and continues to be illuminated with the laser light. If the object under goes a deformation, amplitudes of the two sets of light waves, one being the reconstructed wave and the other the directed wave from the deformed object, will add or cancel depending upon the path difference. As a result the observer viewing the reconstructed image sees it covered with interference fringes. The pattern will be a contour map of the object shape change. A change in the fringe pattern is simultaneously observed with a change in the object - hence the name `real-time' holographic interferometry .

3.2.2 General theory.

Consider an off axis holographic set up. From equation (1.14) the intensity at the holographic plate during recording is

$$I(x,y) = | R(x,y) + O(x,y)|^2$$

$$= | R |^2 + | O |^2 + OR^* + O^*R \qquad (2.1)$$

Assuming a linear recording, from (1.13) the amplitude

transmittance of the processed hologram can be written as

$$T(x,y) = T_o - \beta \tau I(x,y) \qquad (2.2)$$

In real time holography the hologram illuminating waves are the reference wave and the deformed object wave directly coming from the deformed object. Accordingly the complex amplitude of the transmitted wave through the hologram is

$$U(x,y) = \left[O'(x,y) + R(x,y) \right] T(x,y) \qquad (2.3)$$

Here O' is the complex amplitude of the deformed object wave. If this small change in the object shape is assumed as a phase modification $\Delta\phi(x,y)$ of the object wave, then

$$O'(x,y) = |O| e^{-i\phi_0} e^{-i\Delta\phi(x,y)}$$

$$= O(x,y) e^{-i\Delta\phi} \qquad (2.4).$$

Then we can write

$$U(x,y) = \left\{ T_0 - \beta\tau \left[|O|^2 + |R|^2 \right] \right\} O e^{-i\Delta\phi} - \beta\tau O^2 e^{-i\Delta\phi} R^* - \beta\tau |O|^2 e^{-i\Delta\phi} R$$

$$+ \left\{ T_0 - \beta\tau \left[|O|^2 + |R|^2 \right] \right\} R - \beta\tau |R|^2 O - \beta\tau R^2 O^* \qquad (2.5).$$

This transmitted field consists of many waves travelling in several directions. Considering the component waves traveling in the approximate direction of the original object wave alone, we have the first and the fifth terms. These terms create an irradiance that consists of a series of fringes that the eye or the camera sees.

3.2.3. Experimental setup

The holographic setup fabricated has been utilized for the experiment.A 10mw He-Ne laser and Agfa 8E75 plates were used for the recording of the holograms. 10 × 2.5 cm^2 holographic plates cut from the standard plate has been held vertically using a small vice, at the top.The sample film was lightly clamped at both ends by using glass holders, allowing for longitudinal expansion (Fig 3.2).The solution flow arrangement for the *in situ* processing of the hologram can also be seen in the figure. Cadmium sulphide films on 7.5 × 2.4 × 0.05 cm^3 glass substrates, prepared by spray pyrolysis were the first set of samples. Optimum exposure and developing times were found to be two seconds and three minutes respectively. Agfa A903 developer diluted in 1:1 ratio has been used to reduce the developing time and there by the emulsion swelling. On reconstruction very good null patterns were obtained. The film substrate composite was slowly

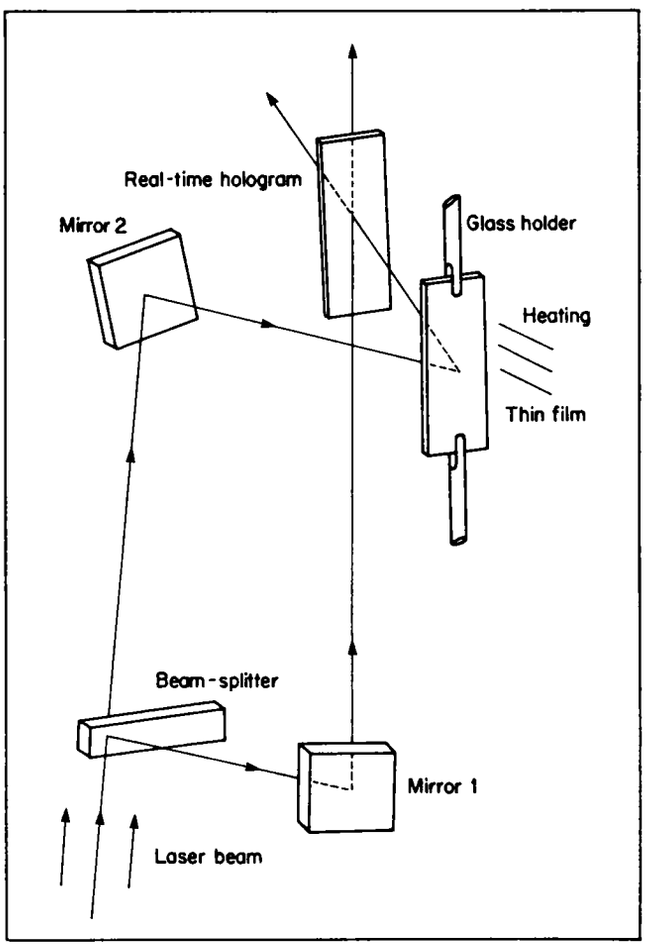

Fig 3.2 Initial setup used for real time holographic stess measurements.

heated, to introduce a deformation, using radiant heating. A heater filament arranged in between two 5mm thick mild steel plates was used for this. The plane of the heater has been kept parallel to that of the film substrate, at a distance of 2mm. The current in the heater has been controlled by using a dimmer-stat. On looking through the hologram we could observe virtual fringes superposed on the film. The fringes remained stationary for a steady temperature. No jitter could be observed under steady air in the room.(This also implies the isolation capability of the vibration isolation table).

In the next set of experiments we have used Ag films deposited on 7.5 x 2.5 x 0.05 cm^3 glass substrates, by vacuum evaporation.Here the beams ratio was set almost equal and the optimum exposure time was 1/5 seconds. On reconstruction,in addition to the common virtual fringes superposed on the sample, as in the case of CdS,which was diffusely reflecting,it was possible to obtain real circular fringes on a screen placed at any plane perpendicular to the ray direction,in front of the hologram (Fig 3.3).These fringes were there both in the reference as well as the object beam directions. The fringes were of very good visibility , compared to common real time holographic fringes.

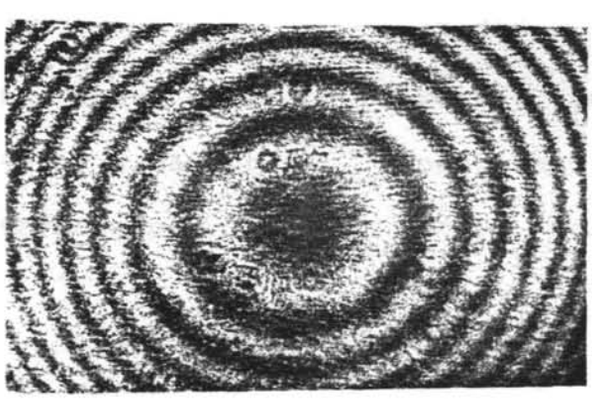

Fig 3.3 Circular fringes generated

3.2.4 Principle of fringe formation.

Since the object is specularly reflecting, an observer at any point in the hologram plane receives wave fronts coming from only one point of the object. The reconstructed wave in one direction will interfere with the corresponding wave in the cone of object waves and causes real fringes on any plane in the object beam direction. If we denote the complex amplitude of the instantaneous object wave reflected by the strained object by O′ then

$$O'(x,y,t) = O(x,y)\exp\left\{-i\Delta\phi(x,y,t)\right\} \qquad (2.6)$$

O(x,y) is the complex amplitude on any hologram point x,y due to the unstrained object and $\Delta\phi(x,y,t)$ is the phase change of the wave due to deformation of the object at any instant t. The reconstruction can represented as :

$$(R + O')T = \left\{T_0 - \beta\tau\left[|O|^2+|R|^2\right]\right\} R - \beta\tau\,|O|^2 e^{-i\Delta\phi}\, R$$

$$+ \left\{T_0 - \beta\tau\left[|O|^2+|R|^2\right]\right\} O e^{-i\Delta\phi} - \beta\tau|R|^2 O - \beta\tau R^2 O^* - \beta\tau O^2 e^{-i\Delta\phi}\, R^* \qquad (2.7)$$

The third and fourth terms in the above equation represent two sets of waves differing in phase by a factor $e^{-i\Delta\phi}$, propagating in the same line, causing interference in the object beam direction.

The deformed object beam O′ reconstructs a correspondingly deformed reference beam represented by $|O|^2 e^{-i\Delta\phi} R$ which interferes with the dc part of the reference beam and produces similar interference fringes in the reference

beam direction also. The last two terms in 2.7 represent the off-axis conjugates.

The theory given in the preceding part gives an explanation for the observation of real fringes in both the object and reference beam directions. Since the object is specularly reflecting these fringes are real and exist in all planes perpendicular to the directions of propagation. By noting the fringe number, deformation of the specimen can be easily observed and photographed, there by stress developed can also be calculated.

A certain amount of external stress can be suspected in the previous experimental setup. This comes due to the way in which the film was held. A new experimental arrangement (Fig 3.4) which avoids possibility of any external stress has been used for the quantitative measurement of the thermal stress.

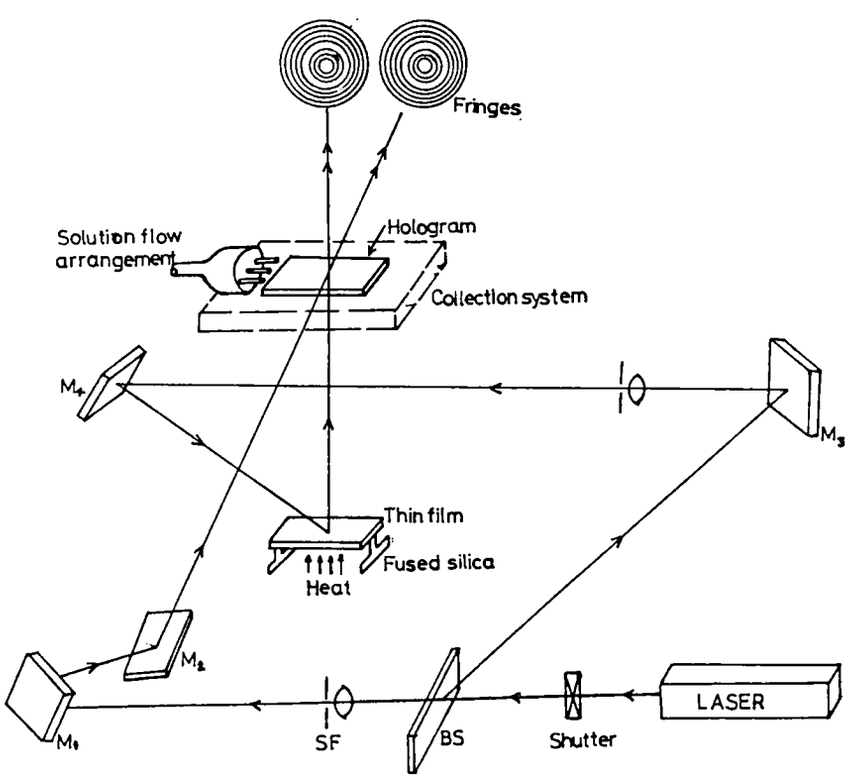

Fig 3.4 New experimental arrengement

Here the sample film was kept freely supported on two 0.6cm wide fused silica knife edges.The holographic plate is held parallel to the film plane by using a small, spring loaded vice, above the sample. The emulsion side of the plate is arranged on the top. A jet like arrangement made with 3mm glass tubes is used for getting a mild,but uniform flow of the solution.The solution flow system is arranged at a height of 25cm above this jet and the hologram. There is a movable solution collection system which can be easily positioned below the holographic plates,even in darkness.Mirrors M_1 to M_4 are used to steer the reference beam and the object beam.

A hologram of the sample film was recorded on the plate and then the solution collection system was arranged below the hologram.After processing, the excess water drops on the hologram were removed first by mild air flow and then with a blotting paper.When the drying was completed, clear, null patterns could be reconstructed. The sample was then slowly heated and the temperature was monitored by using a digital thermometer probe kept just above the sample.Fringes generated from the centre of the specimen and obtained on either beam directions are given in Fig 3.5a and 3.5b.A schematic representation of the wave-mixing is presented in Fig 3.6.

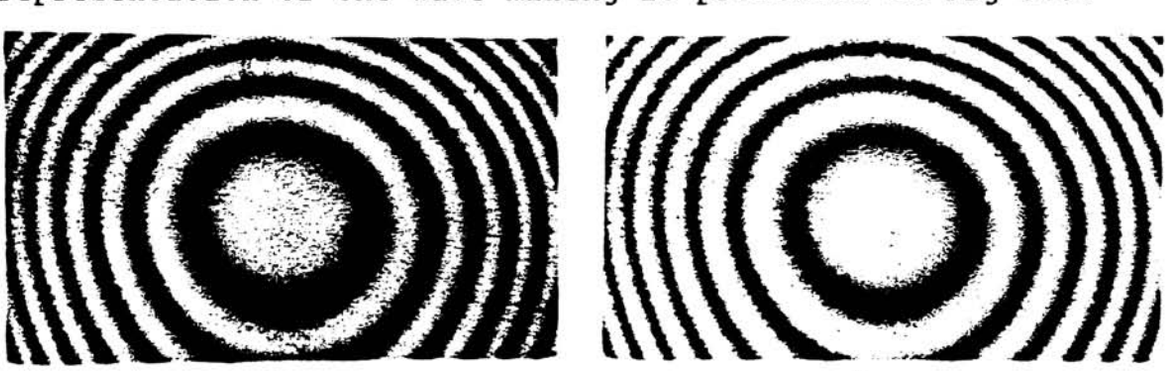

Fig 3.5 Fringes obtained
a. In object beam direction
b. Reference beam direction

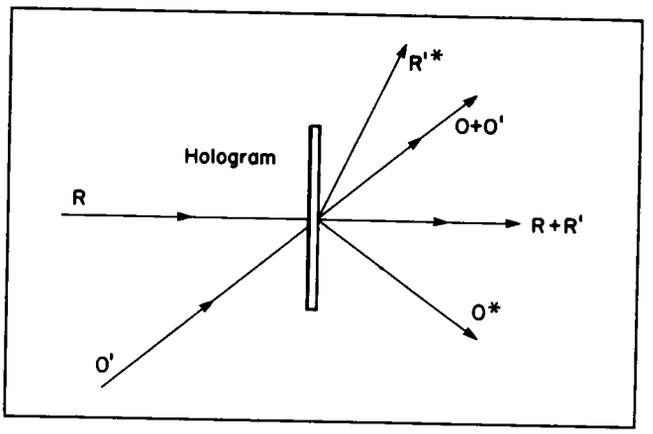

Fig 3.6 Wave mixing

3.3 Calculation of the thermal stress.

By monitoring the fringes, deformation of the specimen and there by the thermal stress S developed for a particular temperature range can be calculated, assuming the film substrate composite as a beam freely supported at its extremities, from the formula [19]

$$S = \frac{4\ Y_s t_s^2 \delta}{3(1-\nu_s)\ l^2\ t_f} \qquad (2.8)$$

The subscripts s and f denote the substrate and the film respectively. Y is the Young's modulus, t the thickness, l length of the composite, ν the Poissons ratio and δ the deflection at the centre produced by the film stress.

Here the deflection has been effected by the thermal stress produced due to the differential expansion of the film and the substrate materials. For 2000^0 A Ag film on 6 × 2.4× 0.015 cm^3 glass substrate, about 21 fringes were obtained in in a temperature range of 27° C to 50° C.This corresponds to a stress of 0.29×10^9 dynes/ cm^2.

The expression for thermal stress [26] is

$$S_T = \frac{Y_f(\alpha_f - \alpha_s)(T_c - T)}{(1-\nu_f)} \qquad (2.9)$$

α represents the linear thermal expansion coefficient, T_c and T are deposition temperature and temperature during the measurement, respectively and ν_f is the Poissons ratio of the film.

Assume that T_H is the temperature at which the hologram is recorded. Then equation 2.9 can be written as :

$$S_{T_H} = \frac{Y_f(\alpha_f - \alpha_s)(T_C - T_H)}{(1-\nu_f)} \qquad (2.10)$$

For any stress measuring temperature T_m

$$S_{T_M} = \frac{Y_f(\alpha_f - \alpha_s)(T_C - T_M)}{(1-\nu_f)} \qquad (2.11)$$

From the above two equations, the predicted value of thermal stress variations for any temperature range T_H to T_M can be written as

$$\Delta S_T = \frac{Y(\alpha_f - \alpha_f)_s (T_H - T_M)}{(1-\nu_f)} \qquad (2.10)$$

For Ag film in the above case $T_H = 27^\circ$ C and $T_M = 50^\circ$C.Then the above expression predicts a stress value 0.33 $\times$ 10^9dynes/cm^2. This agreed well with observed value of 0.29 $\times$ 10^9 dynes/cm^2 , given by equation 2.8.The values of the physical constants

[27,28] assumed for the calculation are presented in the following table.

Material	α_f	α_s	Y_f	Y_s	ν_f	ν_s
Ag	19×10^{-6}	7.4×10^{-6}	7.8×10^{11}	7×10^{11}	0.37	0.35
Cu	17×10^{-6}	7.4×10^{-6}	11.7×10^{11}	7×10^{11}	0.35	0.35
Al	23×10^{-6}	7.4×10^{-6}	6.89×10^{11}	7×10^{11}	0.34	0.35

Since there are only a few wide fringes on the whole length of the test piece, the fringes have been directly read with naked eye. A series of experiments were conducted by using reflecting thin films of Ag, Cu and Al - with different thickness and prepared at different deposition temperatures. All these films were prepared by vacuum evaporation. The deposition temperatures were measured by using a Chromel-Alumel thermocouple. The substrates were thoroughly cleaned by using the procedure described Chapter II. The results of the experiments are presented in the following curves (Fig.3.7).

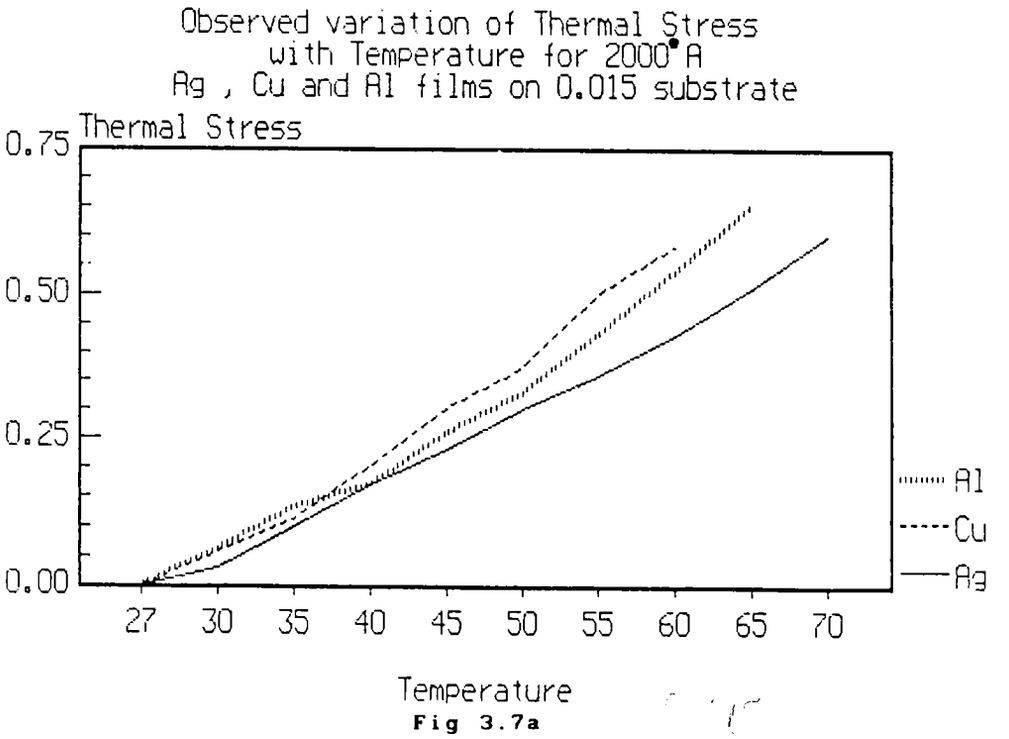

Fig 3.7a

Theoretical Thermal Stress variation

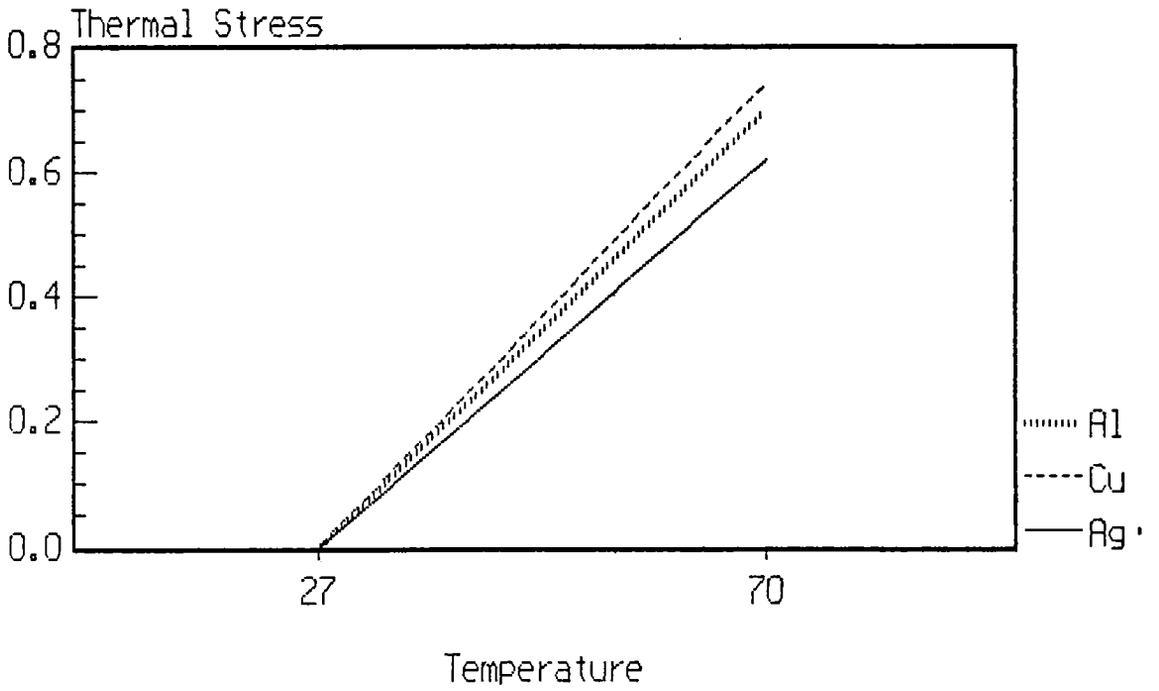

Fig 3.7b

Variation of fringe ordering for 2000 Å Al film on substrates of different thickness

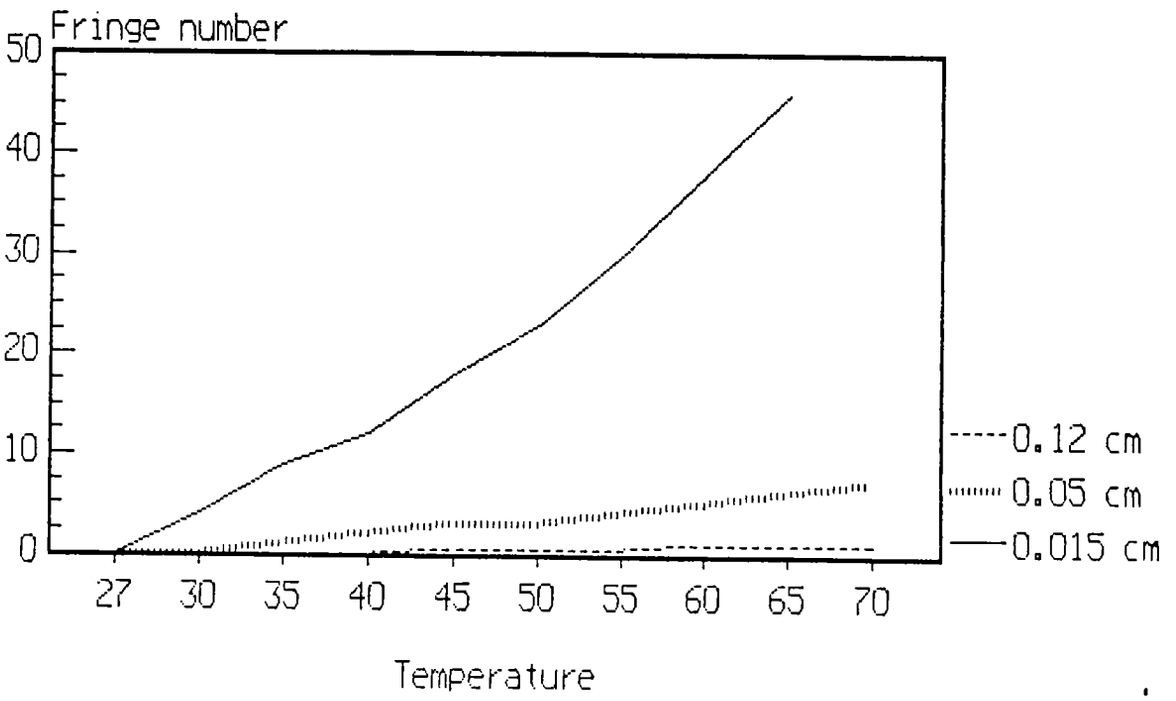

Fig 3.7c

3.4 Results and conclusions.

The real time holographic technique introduced in this chapter is a simple, sensitive and non-destructive method for measuring stress in thin films. Even though only thermally induced stress is discussed here, the technique can be suitably extended to study the development of intrinsic stress during growth, adhesion and film damage by high power lasers. If we take an accuracy of half a fringe for naked eye, in the present experiment, this corresponds to a sensitivity of 7×10^{6}dynes/cm^{2},for a film of 200 nm thickness .The sensitivity of the method depends on the substrate thickness and resolution of the fringe monitoring system. For a higher temperature range an automatic fringe read out system can be introduced.The heating was made slow, ie. about one degree celsius per minute,in order to get a steady fringe system suitable for measurement with naked eye. If the rate of heating is higher, it was found that the fringes moved in a direction which was opposite to the initial fringe movement.This can be explained in the following way. A sudden heating produces temperature gradient across the substrate thickness and the region closer to the heat source will get heated up more. This causes bending of the substrate in a way which is opposite to that produced by the film stress.

Films formed at different deposition temperatures such as 55^{o}C, 65^{o}C and 75^{o}C were used as samples. But any modification in the fringe ordering could not be observed. Al films of thickness 1000, 2000 and 2500Å were also prepared and used as samples. The substrate deformation due to thermal

stress was measured by using the above method. No appreciable variation in the calculated value of the thermal stress could be observed.

Another advantage of the technique over other interferometric methods is that no substrate profile measurement is needed.It was assumed that there is no variation in the intrinsic stress of the film during the above temperature range.

In the case diffusely reflecting CdS films deposited at 300^{0}C on 0.05 cm thick substrate, two wide fringes were obtained for a temperature range of 26 to 50^{0}C .But this stress value could not be verified due to non availability of physical constants of CdS films.

References

1. Horman, M.H, Appl.Opt., **4**, 333, (1965).
2. Powell R.L and Stetson, K.A, J.Opt.Soc.Am.55, 1593 (1965).
3. Powell R.L and Stetson, K.A, J.Opt.Soc.Am. 55, 612A, (1965).
4. Stetson, K.A and Powell, R.L, J.Opt.Soc.Am. 55, 1694 (1965).
5. Burch, J.M, Proc.Eng., **44**, 431 (1965).
6. Stetson, K.A and Powell, R.L, J.Opt.Soc.Am. 55, 1570A (1965).
7. Haines, K.A and Hildebrand, B.P, Appl.Opt., 5, 595 (1966).
8. Brooks, R.E, Heflinger, L.O and Wuerker, R.F, Appl.Phy.Lett. 7, 248 (1965).
9. Stoney, G.G, Proc.Roy.Soc. (London) A82, 172 (1909).
10. Hoffman, R.W, "Physics of Thin Films", Vol.3, p.227.
11. Orlinov, V and Sarov, G, Thin Solid Films, 68, 333 (1980).
12. Dumin, D.J, J.Appl.Phy. 36, 2700 (1965).
13. Toxen, A.M, Phys.Rev. 123, 442 (1961).
14. Notarys, H.A, Appl.Phys.Lett. 4, 79 (1964).
15. Maissel, L.I and Glang, R "Handbook of Thin Film Technology", Chapter 12, p.36, Mc Graw Hill, New York (1970).
16. Glass, A.J and Guenther, A.H, (Eds) "Laser induced damage", NBS, Washington D.C, (1975).
17. Murbach, H.P and Wilman H, Proc.Phys.Soc. (London), B66, 911 (1953).
18. Backburn, H and Campbell, D.S, Phil.Mag. 8, 883 (1963).
19. Ennos, A.E, Appl.Opt. 5, 51 (1966).

20. Finegan,J.D and Hoffman,R.,Transactions of 8th National Vacuum Symposium (Pergamon, New York), p.935 (1961).

21. Vook, R.W and Witt, F, J.Appl.Phy. 36, 2169 (1965).

22. Pashley, D.W, Phil.Mag. 4, 324 (1959).

23. Magill, P.J and Young, T, J.Vac.Sci.Technol. 4, 47 (1967).

24. Ramprasad, B.S and Radha, T.S, Thin Solid Films, 51, 335 (1978).

25. Ramprasad, B.S and Radha, T.S, Appl.Opt. 17, 2670, (1978).

26. Sharma, S.K, and Spitz, J, Thin Solid films, 65, 339 (1980).

27. Hodgman,C.D (Ed.),"Hand book of Chemistry and Physics", The Chemical Rubber Publishing Co.,Ohio,(1963).

28. Gray,D.E (Ed.),"American Institute of Physics Hand Book", Mc Graw-Hill, New York,(1972).

CHAPTER IV

VIBRATIONS OF AIR-REED MUSICAL WIND INSTRUMENTS BY USING TIME-AVERAGED HOLOGRAPHIC INTERFEROMETRY

Abstract

Knowledge of wall vibrations of musical instruments is important for testing the sound quality of a particular instrument as well as for instrument design. The traditional Chladnis method for observing the eigen modes gives only the position of nodal lines, but no amplitude and phase information. Also the technique is not suitable for curved surfaces of musical wind instruments. Introduction of holographic interferometry helped a lot to overcome these drawbacks. But this technique has been mainly used for the analysis of musical string instruments rather than wind instruments, because of problems of stability during excitation. In the case of musical wind instruments the effect of wall vibrations on the tone quality is a much argued question. We have attempted to record the wall vibration of some air-reed flutes by using conventional holography and with suitable excitation process, which we believe, for the first time yielded well defined time-averaged interferograms. This chapter deals with the experimental technique used and the results obtained.

VIBRATIONS OF AIR-REED MUSICAL WIND INSTRUMENTS BY USING TIME-AVERAGED HOLOGRAPHIC INTERFEROMETRY.

4.1 Musical instruments and holography.

4.1.1 Vibrations of musical instruments.

In most of the musical instruments there are sources of vibrations, whose frequency can or can not be varied,coupled to a resonator. The resonator may also be adjusted to vary the frequency.The shape of the resonator and the sound radiating from the wall vibrations of the instrument contribute to the ` colour ' and quality of the total instrumental sound. Considering a particular musical instrument, the contribution from the wall vibration is decisive in distinguishing a great instrument from an ordinary one. Knowledge of the wall vibrations is also helpful in designing good quality musical instruments and to study resonant vibrations of any particular design. It is well known that the properties of ` belly ' and ` back ' (top and back plates) of instruments of the violin family (violin,viola,cello and bass), to a great extent, decided the quality of their sounds. Modern tests of vibrational properties of the top and back plates revealed something of what famous violin makers did by ` feel ' and led to the making of consistently good violins.

Even though every body accepted the contribution of the wall vibrations,no test methods were there to form some

hard and fast rules for the fabrication.For many years the secrets of such great instruments made by Andra Amathi and Stradivarius was a mystery.

A traditional method evolved in 18th century was the technique worked out by Ernst. F. F.Chladni [1]. In this method the normal mode patterns of vibration of a horizontally mounted flat plate are demonstrated by sprinkling the plate with some fine powder and then causing the plate to vibrate.At the eigen frequencies the vibrations bounce the powder into the nodal regions where there are no vibrations. Thus a mapping of the nodal and the anti nodal configurations of the plate at its specific resonance frequencies can be achieved.

Chladnis method provided only the positions of the nodal line, but no amplitude and phase information.More over the technique was not suitable for the curved surfaces of musical wind instruments.Many things regarding music and musical instruments were mysterious and the major advance over the last few decades has been in holography, applied to vibrating surfaces. This method is not only is more sensitive but also indicates motion in the anti nodal areas in the Chladni method.

4.1.2 Time-averaged holography.

In holographic interferometric vibration analysis the wave front reconstruction technique has been used to map the amplitude of vibration and in some cases the phase of a surface too. The commonly used method for this purpose is time-averaged

holographic interferometry [2,3]. Here the hologram is recorded while the object is vibrating.The phase of the object changes very slowly in time compared to that of the electric field of the laser beam . Thus the hologram recording process can be thought of as the recording of a large number of superposed holograms, one for each slightly different position of the object. After a linear recording, the complex amplitudes of the wave reconstructed will be proportional to the time-average of that scattered from the vibrating object, over the exposure interval. Then the image of the surface will be modulated by a system of interference fringes. The brightest fringe coincides with the nodal region and will be similar to that produced by the Chladni method. In time-averaged holography,in addition to the bright nodal fringe, there may be other fringes which are contours of equal vibrational amplitudes. But the relative vibrational phase variation across the object surface is not observed and the fringe visibility decreases with increasing amplitude of vibrations. Also there are other analogous holographic techniques such as real-time [3], stroboscopic [4-6] and the more general temporary modulated [7]holography, with additional experimental complexity.

In 1969 Carl-Hugo Agren and Karl A. Stetson presented [8,9] their work on the first application of vibration analysis by holographic interferometry to the study of stringed instruments. After their studies on classical treble viol they could design a new instrument with very good results. After exhaustive experiments on acoustics of violin plates by using holography C.M.Hutchins [10] concluded that the mode shapes for instruments of the violin family are found to follow a similar

sequence in all sizes of free plates, but the frequencies at which they occur are unique to each plate. He also observed certain relations between the modes which result in a good quality instrument.

4.2 Air-reed musical wind instruments.

There is no doubt that the timber and the musical quality relating to stringed instruments family mostly depend on the resonator and the surface vibrations of its material [8-12]. But in the case of musical wind instruments the effect of wall material and its vibrations on the tone colour and other playing qualities is a much argued question.

4.2.1 Air-reed excitation.

Here a high speed ribbon of air is blown against the edge of a hole in the instrument. The orchestral flute, recorder and organ flue pipe use this excitation mechanism. The air-ribbon may be formed by the human lips (orchestral flute) or from a fixed structure (recorder and organ flue pipe). The former method has greater degree of flexibility in compass,sound level and intonation, because of the possibility of lip adjustments. In many presentations both scientists and musicians are divided in their opinion on the effect due to the contribution of the wall material [11,13-16].

Referring to clarinet, Richardson [14] states that the rigidity of the tube influences damping of the tone and it enhances notes in certain regions of the scale. Jeans and Taylor [11] pointed out the choice of material for an organ

pipe and the influence of the thickness and character of the wood on the *formant*. After carefully constructing identical pipes of different materials, Von Glatter-Gotz [11] in 1935 concluded that the geometrical shape was the only important factor in the tone quality of pipes. But musicians [15,16] claimed without substantiating, that the tone of metal clarinet was vapid and uninteresting. After a set of experiments Parker [17] compared metal and wood clarinets, and stated that under steady state conditions the material had no effect on the tone quality. Backus and Haudley [18] and Clotman [19], found that although the walls do vibrate, these vibrations were insufficient to affect the steady state tone quality of clarinet, organ pipe and flute. We have contacted some of the leading flute players* both in the realms of classical Carnatic music and orchestral music.

In the interviews they have pointed out,apart from the players qualities, the following facts: The material has got a good contribution in the tone quality of the instrument. Even though it is not as prominent as in stringed instruments, it decides to a good extent the sweetness of the tone and ease of play. From their experience they are of the opinion that matured reed is the best material for making flutes.Regarding the thickness: there are two types of blowing, soft blowing and hard blowing. Usually players in the soft blowing school prefer flutes made of thin material and vice versa. They say

---

* 1.Srikrishnan G.S,Carnatic flute player, Assistant Station Director, AIR, Cochin.
2.Ravindranath.K.V,Carnatic flute player,Alleppy.
3.Murali.P.R, Orchestral flute player,Cochin.

that the hard blowing player using a thick flute produces sound with more `depth'.

Without the help of a potential scientific tool to map the surface vibrations of wind instruments,it is a virtually impossible task for the scientist to be able to produce sufficient evidence to show that a player may be wrong in his opinion.

Coming to holography, in their very first paper [2] stating mechanical stability as a crucial parameter, Powell and Stetson suggested its usability only in the case of musical stringed and percussion instruments. Logberg and Ledang [20],after considering the problems of stability during excitation, suggested electronic speckle pattern interferometry (ESPI), for studying wall vibrations of willow flutes. Thus it has been considered that the stability requirement of holographic process limits the effective use of conventional holographic technique in the case of wind instruments, as they are excited by an air-flow, which easily introduces unwanted movements. Moreover an artificial excitation by a transducer may not necessarily represent the actual behavior of the instrument.

4.3 Recording of time-averaged holograms of air-reed flutes.

After considering the above said incertitude we have attempted to record the wall vibrations of some air-reed flutes by using conventional holography. With a suitable excitation process,we could, probably for the first time,get well defined

time averaged interferograms. The Indian flutes we studied were made of a kind of reed of the genus Gramineae whose botanical name is Ochlandra Travancoria. A hollow stem of suitable length cut from matured reed, after traditional ripening processes such as boiling in water,followed by oiling and drying in a gentle flame,is used for making the instrument. This type of flutes although ancient,(in Sharngdeva's *Sangria Ratnakara*,written in 1247 AD, the dimensions of different flutes are mentioned) is still popular for its simplicity and tone quality. Difficulty in the electronic synthesis of its sound is another reason for its popularity. It has no keys and levers and is side blown. A hole at one end near the node of the reed serves as the mouthpiece. Air is blown directly into the hollow of the instrument, against the sharp edge of the mouth hole, upon which the air breaks up into flutters and setting into vibration of the air. There are six finger holes, and mainly the distance of the first finger hole from the mouthpiece decides the pitch of the flute. Two and a half octaves can be easily generated with the instrument. Usually dehydration problems do not arise as the reed is well dried.

4.3.1 Experimental setup and General Theory

During the initial part of the work different mouthpieces capable of producing air jet and air ribbon were made of glass and rubber. Compressed air through a needle valve NV (Fig 4.1) was gently let through the mouthpiece M, using a rubber tube. It has been found that in the case of rubber mouthpieces producing an air ribbon, it was easy to excite the flute even without touching the mouthpiece hole.

The direction and pressure of the air ribbon were adjusted with a precision XYZ-translator arrangement T and the needle valve to obtain a clear sound. The wave pattern produced by the instrument was observed using an oscilloscope and was almost sinusoidal, which was similar to that produced by realistic excitation.

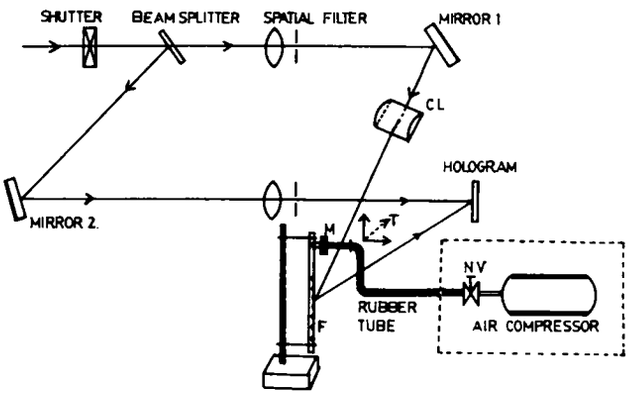

Fig 4.1. Experimental setup for recording the vibration patterns of the flute.

The holographic setup shown in Fig.4.1 is a simple conventional one. A 10 mw He-Ne laser and Agfa 8E75 plates were used for recording the hologram. An uncoated 10 mm thick glass plate (transmissibility of about 90%) was used as the beam splitter (BS). The ratio of energies of the reference field to that of the object field was about 4:1. The entire length of the flute F was illuminated with the help of a cylindrical lens CL. A 20 X microscope objective-pin hole arrangement was used as the spatial filter. The system was mounted on the vibration isolation table described in Chapter II.

At first the flute was lightly clamped at one end near the mouth hole and excited. We could record fringes near the mouth hole Fig.4.2.,similar to those obtained in [20].

Fig 4.2 Fringes near the mouth hole.

Reconstruction of the remaining area was disturbed by stability problems. But when the flute was lightly clamped at either end and excited, which is almost similar to playing conditions, very good interferograms as shown in Fig.4.3.,were obtained for various frequencies. The frequency is changed by closing and opening the holes sequentially.

Fig 4.3 Interferogram of a vibrating flute.

The exposure time was about 5 seconds. If we assume almost pure harmonic vibrations [20-22] then at any point P(x,y) on the flute at time t, the displacement is given by

$$L(x,y,t) = L(x,y) \sin \omega t \qquad (4.1)$$

ω is the angular velocity of the object motion. The phase change of the light wave scattered from this general point is

$$\Delta\phi(x,y,t) = K.L(x,y) \sin \omega t \qquad (4.2)$$

K is the sensitivity vector which points along the angle 2θ between the illumination and viewing directions and its

magnitude is $4\pi \cos(\emptyset)/\lambda$.

If $$O(x,y) = |O(x,y)| \exp[-i\phi(x,y)] \qquad (4.3)$$

is the complex amplitude of the scattered light from the point P, when the flute is stationary. Then, that at any instant during the vibration is

$$O(x,y,t) = |O(x,y)| \exp\{-i[\phi(x,y)+K.L(x,y)\sin(\omega t)]\} \qquad (4.4)$$

Assuming a linear recording process, the complex amplitude U(x,y) of the reconstructed wave will be proportional to the time average of O(x,y,t) over the exposure time T.

Hence

$$U(x,y) = \frac{1}{T}\int_0^T |O(x,y)| \exp\{-i[\phi(x,y)+K.L(x,y)\sin(\omega t)]\}\, dt \qquad (4.5)$$

$$= |O(x,y)| \exp[-i\phi(x,y)] \frac{1}{T}\int_0^T \exp[-iK.L(x,y)\sin(\omega t)]\, dt \qquad (4.6)$$

If the exposure time is longer compared to the period of vibration of the flute ie., $T >> 2\pi/\omega$, then

$$U(x,y) = O(x,y)J_0[K.L(x,y)] \qquad (4.7)$$

where Jo is the zero-order Bessel function of the first kind, defined by

$$J_0\,[K.L(x,y)] = \lim_{T\to\infty} \frac{1}{T} \int_0^T \exp[-iK.L(x,y)\sin(\omega t)]\, dt \qquad (4.8)$$

Then the intensity of the image reconstructed is

$$I(x,y) = I_0(x,y)\, J_0^2[K.L(x,y)] \qquad (4.9)$$

where $I_0(x,y) = |O(x,y)|^2$, the intensity when the object at rest. The zeros of the function $J_0^2[K.L(x,y)]$ correspond to the dark fringes and the first maximum corresponds to the nodal region. Since the amplitude of vibration varies across the object, we will get fringes of equal amplitude vibrations on the object. The bright region represents the node and corresponds to the first maximum of the Bessel function.

4.4 Results and discussion.

The primary aim of the experiment was to demonstrate the capability of conventional holography to study the wall vibrations of air-reed wind instruments, excited in almost realistic playing conditions. It also shows that a compressed air-ribbon can be used to excite the flute, even without touching it and without introducing any stability problems.

Motivated by the initial success in the experiments we have carefully made two sets of identical flutes of different materials viz., aluminium, brass, stainless steel and plastic, and conducted more experiments. The length, diameter and thickness of the two sets were 22, 1.4, 0.18 cm and

24, 1.6, 0.18 cm respectively.Holograms of each flute, excited with one full note frequency difference, covering about two and a half octaves, were recorded.In either of the sets it has been found that in the case of flutes made of reed the surface vibrations were strong enough to get a good number of fringes (Fig 4.4), in the higher octave region. But in some of the lower octave notes we could observe only one or two fringes, implying a lesser contribution from the surface. Fig.4.4a. represents the vibrations on the flute when all the finger holes were kept open. Fig.4.4b. represents those when all the finger holes except the first was kept open. Fig.4.4c and Fig.4.4e. represent the vibrations on the flute surface when the first two and first three finger holes were closed. The nodal region comes just above the second closed hole from the open one. It is known that apart from the column length, the frequency of oscillation depends on air velocity [11]. Fig.4.4c and 4.4d show the reconstructions with the same column length but the pressure was slightly increased in the latter case. Fig.4.4f is the reconstruction when all the finger holes except the first were closed.Reconstruction of another flute made of reed and is a memeber of the second set, excited at various frequencies are given in Fig.4.5.

In the case of plastic flutes the fringe number was less even in the higher octave, compared to the reed flutes. But when thickness was reduced to 0.7 mm, we could observe a good number of fringes (Fig.4.6).

a

b

c

d

e

f

Fig 4.4 Time averaged holographic reconstructions for various frequencies of the flute made of reed. a.2350 Hz., b.2560 Hz., c.with the same column length as in (b) but with blowing pressure slightly increased, d.2800 Hz., e.3200 Hz., f.3400 Hz.

a. 1940 Hz

b. 2350 Hz

c. 2350 Hz (back side)

c. 2560 Hz

Fig 4.5 Reconstructions of another flute made of reed (member of the second set) for various frequencies

a. 1600 Hz

b. 1750 Hz

c. 1940 Hz

d. 2000 Hz

e. 2350 Hz

f. 2560 Hz

g. 2800 Hz

h. 3200 Hz

Fig 4.6 Reconstructions obtained in the case of 0.07 cm thick plastic flute

In the next set of experiments we have used Brass, Stainless Steel and Aluminium flutes. No fringes could be observed even at the highest note. The thickness was then reduced to 0.7 mm and again the entire experiments were repeated. Then also we could not observe any surface vibrations except in the case of Aluminium flute, at a frequency 2800 Hz. This fringe structure was regular (Fig.4.7)

Fig 4.7 Only surface vibrations observed in the case of thinned aluminium flute at a frequency of 2800 Hz.

and was similar to that obtained for reed flute (Fig.4.5) at a frequencies of 2560 and 1940 Hz.The regular patterns repeated in the cases of the flutes also, but these mode patterns occurred at different frequencies.

Thus it can be concluded that flutes made of reed have got better surface vibrations compared to flutes made of other materials, which might explain the richer sound from a natural reed flute as claimed by the musicians.That is wall vibrations from the material of a wind instrument give a contribution to the total sound quality, which may be decisive in distinguishing a great instrument from an ordinary one. But this contribution is not as prominent as in the case of stringed instruments. The contribution from the surface vibrations is more in the upper octave region. Metallic flutes show almost no surface vibrations.

Considering the sounds of these flutes in the steady state conditions, appreciable difference in quality could not be observed to an untrained ear. But while playing,the difference may be more explicit as claimed by musicians. Let us consider two more facts. Even for an untrained listener there is no doubt that the sound of the flute of some Carnatic musicians is more sweet, even though all of them use reed flutes. Even if their blowing methods and other variables like pressure volume etc., are taken into account, the players agree on one thing that certain flutes have better quality sound compared to others made of the same material. These facts together support the contribution from the surface vibrations.

It is also found that thin flutes contribute more from the surface vibrations. This may also be related to the rich sounds of thinner flutes as the players claim, compared to the thicker ones, which has to be hard blown to produce sound with a better depth.

The existence of relations between the modes as in the case of good violins [10] is yet to be checked in the case of great flutes. It is clear that the opinions of musicians, even after considering the chances of prejudices, both from the East and West, are true in some aspects which we have checked. The better surface vibrations in reed flutes may be explained in terms of the texture of the material. In some of the initial experiments we have used real-time holograms and the flutes were excited using the vibrations from a loud speaker. Some modes were found in between the frequencies produced by the finger holes. This also supports the difference in sound quality between steady state conditions and playing.

The flutes we use, nowadays, are developed versions of the early type made by primitive man. This type of instruments may be the simplest in any symphony orchestra (apart from the stick in the hands of the conductor). The sound generated by wind from a beetle-made hole on a reed might have aroused wonder in a primitive man. In these modern days of electronic revolution, many aspects about that wonder still remain both in synthesis and analysis. Even though we have not done any acoustical analysis of the instrument, by using holography, we hope that more experiments with a few ` great flutes ' might reveal more about it, leading to better understanding and design of this instrument.

References

1. Rossing, T.D, Am.J.Phys. 50, 271, (1982).
2. Powell, R.L. and Stetson, K.A, J.Opt.Soc.Am. 55, 1563 (1965).
3. Stetson, K.A and Powell, R.L, J.Opt.Soc.Am. 55, 1694 (1965).
4. Archbold, E and Ennos, A.E, Nature, 217, 942 (1968).
5. Sajanko, P and Johnson, C.D, App.Phys.Lett. 13, 22 (1968).
6. Watrasiewicz, B.M and Spicer, P, Nature, 217. 1142 (1968).
7. Aleksoff, C.C, Appl.Opt. 10, 1329 (1973).
8. Agren, C.H and Stetson, K.A, J.Acoust.Soc.Am. 46, 120(A) (1969).
9. Agren, C.H and Stetson, K.A, J.Acoust.Soc.Am. 51, 1971 (1972).
10. Hutchins, C.M, Sci.Am.,245, 127 (1981).
11. Smith, R.A and Mercer, D.M.A, Rep.Prog.Phys., 42, 1085 (1979).
12. Raman, C.V, Phil.Mag. 32, 391 (1916).
13. Miller, D.C, "The Science of Musical Sounds", Macmillan, London (1926).
14. Richardson, E.C, "The Acoustics of Orchestral Instruments and of the Organ, Arnold, London (1929).
15. Baines, A, "Woodwind Instruments and their History, Faber, Lodnon (1962).
16. Rendal, F.G, "The Clarinet, Benn, London, (1957).
17. Parker, S.E, J.Acoust.Soc.Am., 19, 415 (1947).
18. Backus, J and Hundley, T.C, J.Acoust.Soc.Am. 39, 936 (1966).
19. Coltman, J.W, J.Acoust.Am. 44, 983 (1968).
20. Lokberg, O.J and Ledamg, O.K, Appl.Opt. 23, 3052, (1984).
21. Vest, C.M.,John Wiley and Sons,New York, (1979).
22. Hariharan, P.,"Optical Holography", Cambridge University Press, New York, Chapter 15, p 234, (1984)

CHAPTER V

HOLOGRAPHIC OPTICAL ELEMENTS AND PATTERN RECOGNITION

Abstract

As a result of extensive research and development during the last twenty years holographic optical elements (HOEs) have become practical and are used in many applications. By using the fabricated experimental setup, we have attempted to record a few simple HOEs, in our laboratory. Combining a matched spatial filter and a holographic lens on a single Agfa 8E75 plate, a compact optical frequency plane correlator has been developed for pattern recognition. The recording details of the HOEs and the pattern recognition system are discussed in this chapter.

HOLOGRAPHIC OPTICAL ELEMENTS AND PATTERN RECOGNITION

5.1 Introduction

Optical elements can be generally categorised into three basic types, viz reflecting elements, refracting elements and diffracting elements. Holographic Optical Elements (HOEs) come in the last set. In its structural sense a hologram can be considered as a record of a set of interference fringes formed between two mutually coherent beams. This system of fringes forms a complex grating which diffracts light falling on it and transforms a part of the light into a desired image. Using this technique it should also be possible to reconstruct the wave fronts coming from lenses, mirrors or gratings. Such holograms can replace some or all the optical elements in a system.

Though the seeds for the conceptual development of HOEs were sawn by Dennis Gabor himself [1-3], it can be considered that the interpretation of holograms by Rogers [4] as a generalised zone plate has laid the foundation for the development of HOEs. In 1966 Kock et al. [5] analysed the imaging property of the hologram of a point source of light and its function as a lens was experimentally demonstrated by Schwar et al. [6].

Holographic counter parts of conventional optical elements have been investigated by many people. To name some -

Denisyuk [7], Mintz etal.[8], Gupta and Aggarwal[9],simulated a few holographic mirrors. Kogelnik [10] and Gavrilov et al. [11] reported holographic simulation of beam-splitters/ combiners. Kogelnik [12], Murty and Das [13,14] Hayat and Pieuchard [15] described construction of holographic diffraction gratings. Since its practical realization, a burst out in the literature regarding HOEs has occurred. Mosyakin and Sarotskii [16], Close [17] and Chang and Winick [18] attempted to present reviews on the state of the art, bearing on the subject. Lerner et al.[19] have done a review of diffraction gratings, ruled and holographic. Ananda Rao and Pappu [20] treated a complete set of configurations for the simulation of different types of mirrors.

Holographic optical elements are unique in many of their characteristics. As we have seen they are diffractive elements and hence wavelength sensitive. HOEs can serve multiple functions viz., as a lens, beam splitter and spectral filter, at the same time. The flexibility in fabrication and possibility of replication along with their added advantages such as lightness and compactness gave them increasing popularity.

The ratio of the hologram thickness to the fringe spacing determines whether a hologram is thin or thick. The interference pattern recorded in a holographic material may be either a spatial variation of absorptiveness, thickness or refractive index. Holographic optical elements of the first type are absorption elements and those of the second and third type are phase elements.

The performance of a HOE is basically determined by its aberrations and diffraction efficiency. The directions of the diffracted rays (as given by the grating equation) are determined by the surface fringe structure and hence the aberration performance depends on the hologram surface fringe structure [18] For considering the recording of a generalized grating, we take object wave O $\exp(i\phi_0)$ and the reference waveR $\exp(i\phi_R)$. Then the amplitude transmittance of the recorded hologram may be written as

$$T = \beta\left[|O|^2 + |R|^2 + 2OR\ \mathrm{Cos}(\phi_0 - \phi_R)\right] \qquad (5.1)$$

Illuminating the hologram with a reconstruction wave C $\exp(i\phi_C)$, we get

$$I = \beta\left[C|O|^2 \exp(i\phi_C) + C\,|R|^2 \exp(i\phi_C) + COR \exp i(\phi_C + \phi_0 - \phi_R)\right.$$

$$\left. + COR \exp i(\phi_C - \phi_0 + \phi_R)\right] \qquad (5.2)$$

The first two terms in the above equation forms 'dc' bias and the third and fourth terms create the virtual and real images respectively. The position and the shape of the fringes formed in the hologram is determined by the phase difference between ϕ_0 and ϕ_R.

The main task of a HOE designer is to determine an optical system, which can holographically produce a HOE, having a surface and internal fringe structure which is compatible with the desired aberration and diffraction efficiency. For the fabrication of high quality HOEs the construction optics

should also be of high quality. Any defects in this optics will be recorded in the HOE. Multiple reflections between the surfaces of the construction optics and scattered light should be minimized. Extreme mechanical stability of the optics and the supporting surface is required. The system should also be kept free from dust and other noise sources.

By using the fabricated experimental setup, we have attempted to record a few holographic lenses, mirrors and gratings. Then a pattern recognition system which uses conventional glass lenses has been developed. Matched filters [21] for complex spatial filtering have been recorded and the correlation peaks are observed. In the next step a multiple HOE which functions simultaneously as a matched filter and as the second Fourier transform lens has been recorded. The correlation peaks are again obtained.

Only simple methods have been used for the simulation of the above elements and no thorough evaluation of the qualities of the HOEs recorded has been done. Considering the interests developed for the past few years on HOEs we think that the experience we gained, however small it may be, through the fabrication of these elements will be rewarding.This is reported just for completeness of presentation of the work we have done in this field.

5.2 SIMULATION OF HOEs

5.2.1 Holographic Lens

A holographic lens can be considered as an interferogram formed by a spherical wave from a point source and a plane wave reference. When functioning as a lens, the plane wave reference is the lens input, and the focus is the real image of the point source. An off axis arrangement as given in Fig 5.1 was used in our laboratory for the simulation of holographic lenses.

The beam from a 10 mw He-Ne laser is split by using the beam splitter BS of about 50% reflectivity. The spatial filters (SF) consisting of 20 X microscope objectives and pin-holes of about 20 microns diameter are arranged after the mirrors M_1 and M_2 to increase the uniformity of the beams. The pin-holes used here are some of the smallest pin-holes we have made. This has been used to achieve a sharp focus [22,23]. Lens L_2 with a focal length 25 cm has been used for

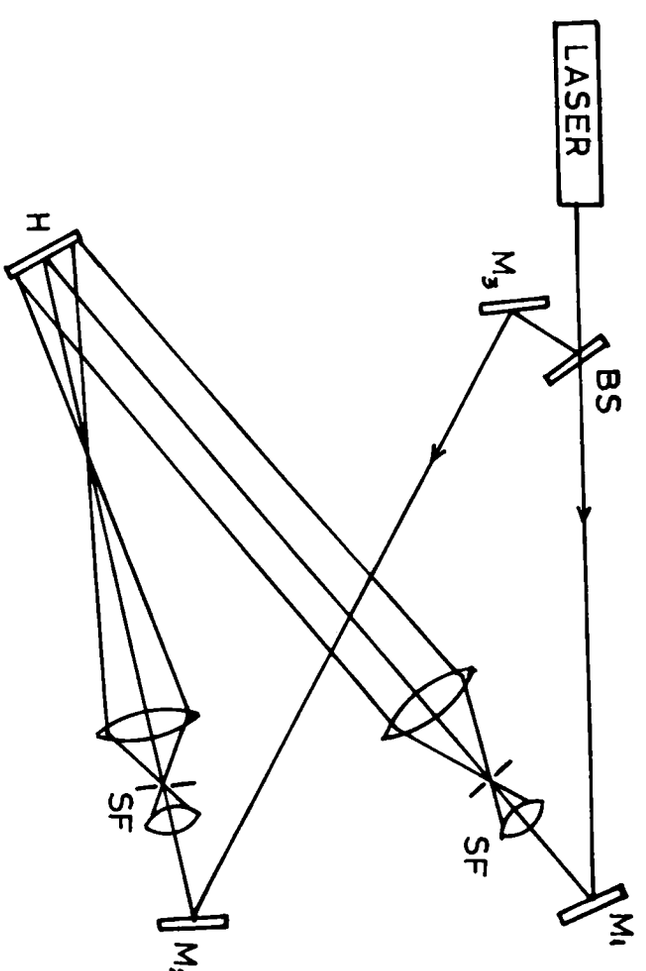

Fig 5.1 Experimental arrangement for the simulation of holographic lens.

collimating the reference beam. The path lengths of the two beams were arranged equal. Fifteen holographic lenses with focal lengths ranging from 10 cm to 30 cm were recorded by using different system configurations. Also the angle between the beams was varied in a range of 10 to 20°. Agfa 10E-75 plates were used as the recording material. During recording the holographic plates were arranged in such way that the two beams made almost equal angles with the plate normal. This has been done in order to minimize the aberrations [23,24] due to emulsion shrinkage. Emulsion shrinkage was also minimized by deliberately over exposing the plate [23]. This reduces the developing time, thereby reducing the emulsion distortions. The exposure time was about 0.1 sec and 1 minute developing was done in 1:1 diluted IPC 163 developer. The effective aperture of the lenses varied from 2 cm^2 to 5 cm^2.

After the usual processing, the lenses were bleached for 3 minutes in 5% aqueous solution of potassium ferricyanide [25] to enhance the diffraction efficiency.

Fig 5.2 shows the reconstructed real focus of one of the holographic lenses with a focal length of 35 cm. The intensities were measured by using the EG & G 460-1A laser power-meter and the diffraction efficiencies were calculated. The best efficiency we could obtain was about 4%.

Fig 5.2 Real focus of a holographic lens.

One of the holographic lenses has been used for

obtaining the Fourier spectrum of a wire mesh. Fig.5.3a and 5.3b are that obtained with a good quality glass lens and with a hololens respectively. The focal length of the two lenses were equal to 25 cm. The quality of the Fourier spectrum

Fig 5.3 Fourier spectrum of a wire mesh formed by

a.Glass lens, b.Holographic lens.

obtained with the hololens is comparable to that obtained with the glass lens.

5.2.2 Holographic Paraboloid Mirrors

In recent years the importance of conic mirrors have got a revival due to their many new applications [8,9] such as spacecraft observatory, spectro-radiometers, laser fusion target illumination systems etc. The fabrication of such mirrors are difficult by using conventional methods. The attractive features of holographic optical elements can be utilized here and the wave front reconstruction technique can be applied to simulate different types of mirrors. Here the holographically simulated mirror (HSM) should reconstruct say, the object wave by reflection. Reflection holograms [25] can

be made by allowing the two beams to enter the emulsion from opposite sides. Different isophase layers will be formed parallel to the hologram surface and the waves reflected by these layers reconstruct the object wave. Reflection holograms of the volume phase type fabricated with dichromated gelatin have efficiencies close [26] to 100%. Holo-spherical mirrors with dimensions larger than 32 inches are used in optical simulators for the training of pilots.

Any general conic section may be represented by the equation

$$y^2 = 2px + (e^2 - 1)x^2 \qquad (5.3)$$

Here e is the eccentricity and 2p is the latusrectum. If we slowly vary the value of e from e > 1 to e = 1, the situation arisen can be analysed as follows. As e comes closer to unity, the second vertex of the hyperbola will be farther from the first vertex (similar is the case with a second branch) and in the limit the hyperbola reduces into a parabola [20]. The situation can be practically realised by mixing a set of plane waves and a set of spherical waves entering the emulsion from opposite sides [20,25]. The traces of the contour surfaces resulting from the interference will be parabolas, almost parallel to the hologram surface. This family of partially reflecting parabolae function as several layers of parabolic mirrors having a common focal point.

The experimental arrangement we have used is given in Fig.5.4. Here a diverging beam and a plane beam are made to enter the emulsion from opposite sides. The two interfering

beams are offset by an angle ϕ = 7° .The holographic plate is kept at the bisector of the angle made by the interfering beams. Seven paraboloid mirrors with focal lengths 15, 20, 25 and 30 cm were simulated. These HSMs were bleached as described in the previous section. A photograph of the reconstructed real focus is given in Fig.5.5.The diffraction efficiency was measured and was found to be only 0.76 % .

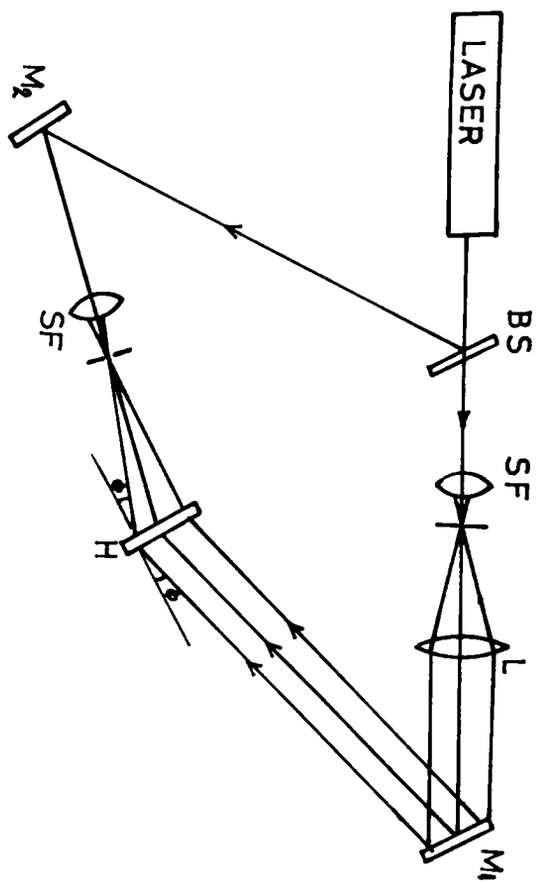

Fig 5.4 Experimental arrangement for the simulation of holographic paraboloid mirrors.

Fig 5.5 Real focus of a paraboloid mirror

5.2.3 Holographic Gratings

Like other HOEs holographically simulated diffraction gratings (HSDGs) have also become a potential tool for instruments designers. Even though the efficiency of HSDGs are not as good as that of ruled gratings [19], their large size, number and pattern of grooves, low scattered light and the freedom for aberration correction make them attractive.

A holographic grating is an interference pattern containing a great number of closely packed fringes. A plane grating is obtained if the interfering beams are plane and the recording of the fringes are done on a plane surface. The theory of HSDGs, their efficiency and aberrations have been discussed by several scientists viz., Kogelnik [12] Murty and Das [13], Noda et al. [27] and Mahipal Singh [28]. The scattering of input light caused by the granular structure of the recording materials and its influence on the diffraction efficiencies of planar gratings have been investigated by Syms and Solymar [29,30].

Consider the simple case of two plane waves derived from a coherent source and the beams intersect at an angle $2\emptyset$. In the region of interference the intensity will be a maximum at the points where the relative phase difference of the waves, say $\phi_2 - \phi_1$, satisfy the condition

$$\phi_2 - \phi_1 = 2n\pi \qquad (5.4)$$

As the plane waves progress in the direction of their wave normals, the interference lines will generate planes of

maximum intensity. These planes of maximum intensity bisect the angle between the wave normals. The period of the sinusoidal intensity variation 'd' is given [25] by

$$2d \sin(\emptyset) = \lambda \qquad (5.5)$$

The period of the fringes decreases with the increase of the angle $2\emptyset$.. If we place a thin photographic material which can resolve 1/d fringe pairs/unit distance, with its plane perpendicular to the bisector of the angle $2\emptyset$, the photographic record of the interference lines (hologram) will function as a HSDG. The grooves in relief produced in the emulsion after processing will be equidistant. Imperfections, roughness etc.. are very much less compared to the ruled grating, thus reducing stray-light.

The arrangement used in our laboratory to simulate a few holographic diffraction gratings is as shown in Fig.5.6. By using a 50% reflectivity beam splitter BS the beam from the laser is divided into two parts. The spatial filters SF are arranged after the mirrors M_1 and M_2 to enhance the beam uniformity. Both the beams are then collimated by using two good quality lenses of focal lengths 25 cm each. Path lengths of the beams were arranged equal.

The photograph of the interference pattern was recorded on Agfa 10E75 plates. Three sets of gratings were simulated by changing the angle between the beams viz., 10^0,15^0, 20^0. The fringe frequency in each case was measured by using a spectrometer and was found to be 273, 414 and 540 lines/mm respectively. The diffraction efficiencies of these

gratings were measured and the best value we could obtain was 3%.

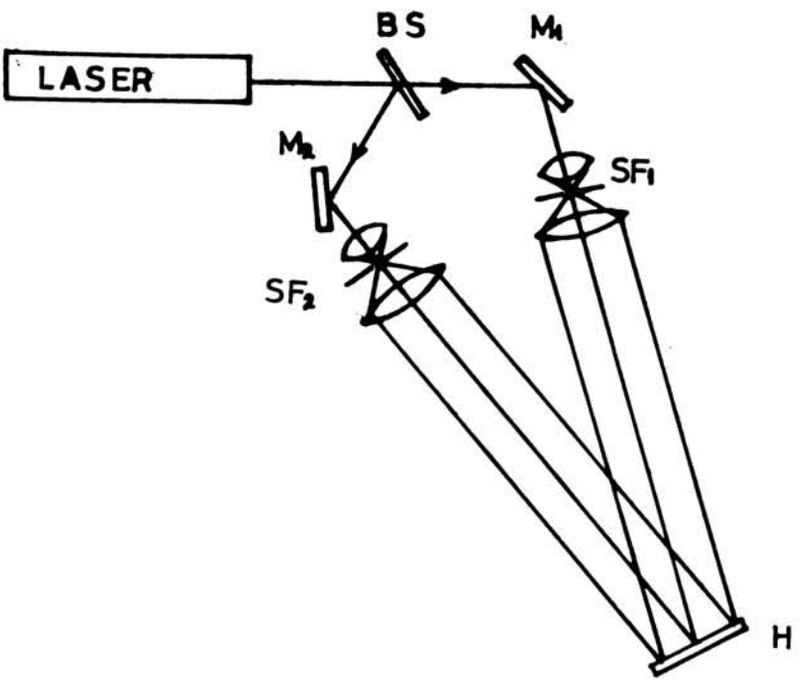

Fig 5.6 Experimental arrangement for the simulation of holographic grating

The diffraction orders of a laser beam, produced by one of the gratings (2Ø = 15) and that of a ruled grating are given in fig.5.7a and b. It can be clearly seen that the stray light because of non-periodic errors [19] in classically ruled grating, is not at all a problem in the holographic grating.

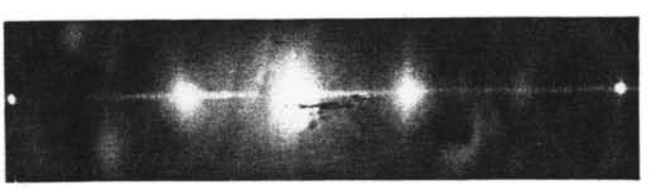

Fig 5.7 Diffraction orders of a laser beam formed by a.Ruled grating

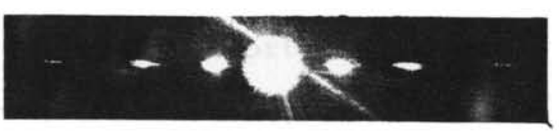

b.Holographic grating

5.3 HOLOGRAPHIC PATTERN RECOGNITION SYSTEM

5.3.1 Introduction

From the lonely domain of lens designers and astronomers optics has now become a vital field affecting all areas of basic research and applied technology. Lasers, holography, optical Fourier transformations and optical spatial filtering are a few of the key items that spawned lots of developments in optics. Optical spatial filtering is one of the most significant developments evolved due to the happy marriage of communications theory and optics [31].

In 1964 Vander Lugt [21,32-33] succeeded in the optical realization of a complex matched spatial filter by combining the concepts of radar processing and holography. Pattern recognition is the identification of a given pattern of data with in a mass of extraneous signals. Considerable research has been done for military applications, but recent advances suggest development of systems with potential commercial applications. An updated summary of the present status of optical data processing has been treated and reviewed by Casesent[34-37]. The rapidly of processing data in parallel and in real time has captured the imagination and brought out the inventiveness of many researchers [38-44]. A holographic technique which can detect and identify images of target objects despite distortions in image scale, angle of view or rotation was reported [45] in 1986. This method, developed at the Imaging Technology Division of Sandia National Laboratories, is effective even if the target is partially obscured. Over the past five years interest in Optical Pattern

Recognition appears to have still increased. Tien-Hsiu Chao and Hua-Kuang Liu [46] reported the use of coherent optical correlation technique for real time tracking of multiple objects making independent movements. Recently a special issue of Optical Engineering [47] which puts together the current research activities on optical pattern recognition has appeared. Various theoretical issues related to correlation filters and important aspects related to practical implementation of correlators are discussed in it.

5.3.2 Initial Experimental Setup and the Basic Principle

Using glass lenses as the Fourier transform elements we have initially constructed an experimental optical correlator as shown in Fig.5.8. The variable beam splitter VBS

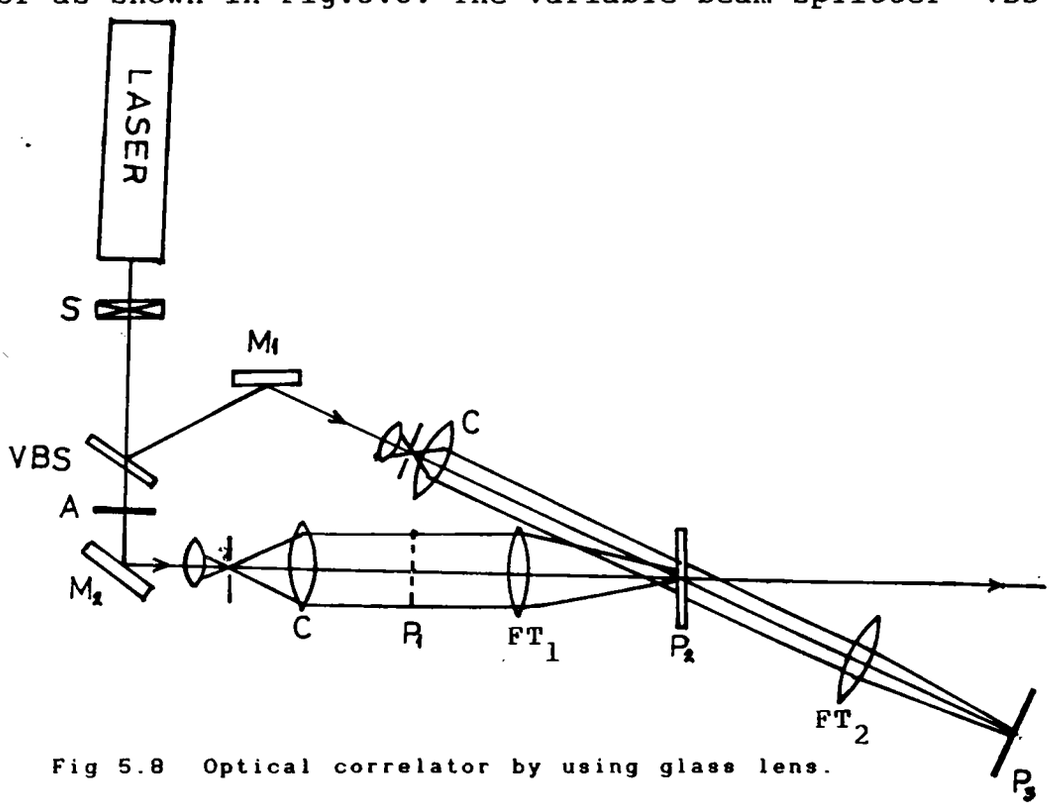

Fig 5.8 Optical correlator by using glass lens.

enables control over the beam balance ration. The folded paths from VBS to mirrors M2 and M1 are used to maintain equal beam path lengths. The angle between the beams is arranged to be

$\emptyset$ = 20°.A variable attenuator A is also arranged in the object beam path to facilitate its intensity variation. S is a mechanical shutter with 'T' setting and having a maximum speed at 1/150 sec. Two spatial filters consisting of 20 microns pinholes and 20X microscope objectives are arranged after the mirrors M1 and M2. Two lenses (L1 and L2) with focal lengths 25 cm and 15 cm are used for collimating the object beam and the reference beam respectively. Lenses FL1 and FL2, both of focal lengths f = 40 cm are used as the Fourier transform elements. The solution flow system described in Chapter III has been used for the *in-situ* processing of the hologram.

We represent the input, transform and output correlation planes by P1,P2 and P3 respectively with spatial coordinates. (x_1,y_1),(x_2,y_2) and (x_3,y_3).If λ is the wavelength of the laser used we can denote the spatial frequency coordinates of the transform plane $(u,v) = (x_2/\lambda f_1, y_2/\lambda f_1)$, f_1 is the focal length of the FT lenses. We use the upper case variables to denote the Fourier transform of the spatial functions. Suppose we initially form a matched spatial filter of the spatial function $h(x_1,y_1)$. This can be done by placing $h(x_1,y_1)$ at the plane P1 and taking hologram of its transform H(u,v) formed at the plane P2 by FL1. After the processing we block the reference wave and a transparency with amplitude transmittance of $g(x_1,y_1)$is placed in the input plane looking for the correlation.

The light distribution $U_2(x_2, y_2)$ in plane P2 due to the complex Fourier transform of $h(x_1,y_1)$ can be represented [25] by

$$H(u,v) = \frac{1}{i\lambda f_1} \iint h(x,y)\exp[-2\pi i(ux+vy)]\, dxdy \qquad (5.6)$$

The light amplitude at the hologram forming plane P2 due to a plane reference wave incident at the angle Ø to the signal beam can be represented by

$$U_R = R_0 \exp(-i2\pi\alpha x_2) \qquad (5.7)$$

where the spatial frequency α associated with the reference wave = $\sin(\text{Ø})/\lambda$. After the hologram recording and processing its transmittance is.

$$T(x,y) = |U_2 + U_R|^2$$

$$= R_0^2 + |H|^2 + R_0 H \exp(i2\pi\alpha x_2) + R_0 H^* \exp(-i2\pi\alpha x_2) \qquad (5.8)$$

In the second stage we block the reference beam and if we keep the transparency $g(x_1,y_1)$ at P1, then the amplitude distribution falling on the hologram in plane P2 is G(u,v) and that leaving the plane is G(u,v) $T(x_2,y_2)$. Lens FL2 then forms the Fourier transform of G(u,v) $T(x_2,y_2)$ at its back focal plane,or finally we get [49] in the plane P3.

$$U_3(x_3,y_3) = R_0^2 g\delta(x,y) + [h \otimes h \otimes g]\delta(x,y) + R_0[h * g * (\delta(x_3 + \alpha\lambda f_1, y_3)]$$
$$+ R_0[g \otimes h * \delta(x_3 + \alpha\lambda f_1, y_3) \qquad (5.9)$$

* implies convolution and ⊗ implies correlation.

The first two terms will be centered on-axis in the plane P3. The third term, the convolution, starts from P2 at an

angle Ø and appears at $(0,\alpha\lambda f_1)$ in the output plane P3. The last term containing the correlation emerges from the plane P2 at an angle -Ø and appears at $(0,-\alpha\lambda f_1)$ in the output plane P3. If the function g contains the reference signal h, then a bright spot of light in the output plane P3 appears due to the correlation. The location of this spot in plane P3 is proportional to the location of the reference function $h(x_1,y_1)$ in the input function $g(x_1,y_1)$.

In our experiments the reference function used was the word HOLOGRAPHY (Fig.5.9). In actual experiments the hologram recording position was slightly defocussed by about 2 cm(about 5% of f1) to improve the dynamic range [49] of the recording medium. The recording medium used was Agfa 8E75 plates which had got a resolving power of about [25] 3000 lines per mm.

Fig 5.9 Reference function

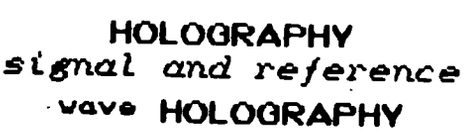

Fig 5.10 Input function.

This type of plates [50] provide uniformly good diffraction efficiency in a spatial frequency range of 500 to 2500 lines/mm. The exposure time given was 1/25 sec. One minute developing was done in IPC 76 fine grain developer. The correlation plane pattern obtained when as input transparency as shown in Fig.5.10 has been used is given in Fig.5.11 The locations of the correlation peaks are proportional to the locations of the word HOLOGRAPHY. The spots with lesser intensity are the erroneous cross correlations. This is due to

the similarity in the general shape of the letters. Binns et al. [39] suggested the use of high signal to reference beam intensity ratios to increase the discrimination between similar patterns.

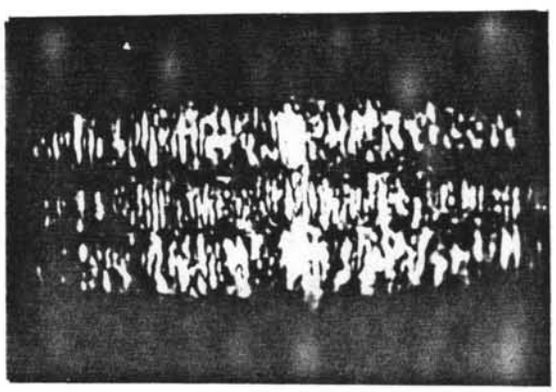

Fig 5.11 Correlation plane pattern.

5.3.3 A Compact Optical Correlator

In any optical frequency plane correlator, its size and weight are two important features [23,48] which have to be considered. Both of these parameters can be reduced by combining the matched spatial filter and the Fourier transform lens on a single plate [48]. For this a multiple function holographic optical element has to be recorded. Fig.5.12a.shows the arrangement for the experimental realization of the above said factors, resulting in a compact optical frequency plane correlator. This is similar to the conventional system described in Fig.5.8 except in the fact that a converging reference beam is used rather than a plane wave. This results in the recording of the matched filter and the Fourier transform lens on the same plate.Lens CL_2 has been kept at a distance of 56 cm from the hologram.

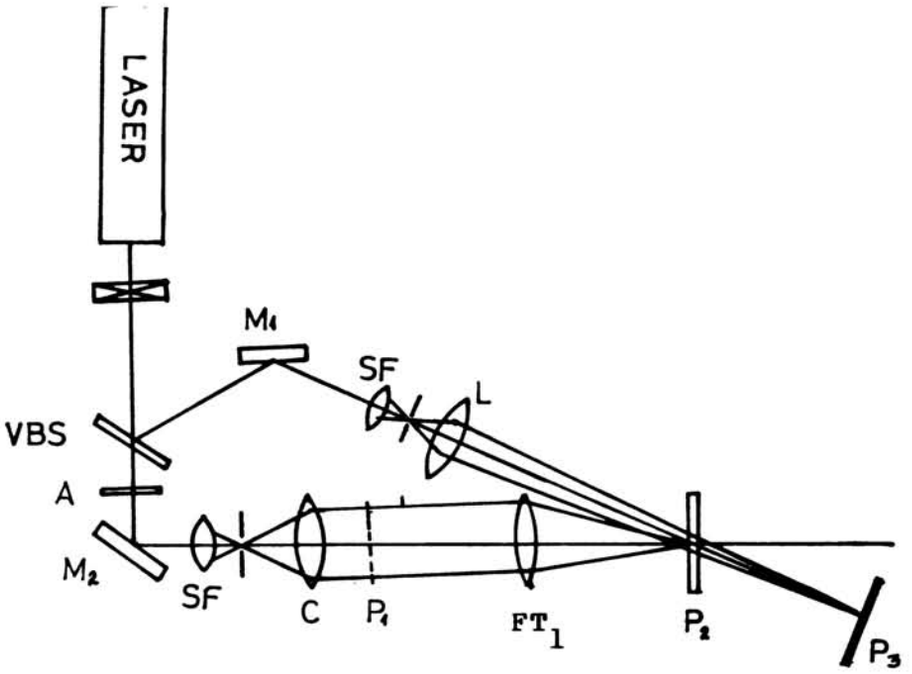

Fig 5.12 a. Compact optical correlator

Same signal and reference functions as in the previous case are used here also . Photograph of the output correlation plane pattern obtained is given in Fig 5.12b.

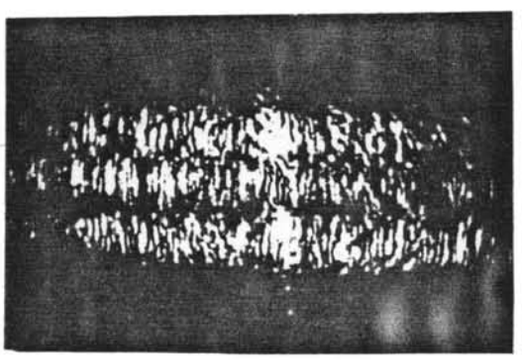

Fig 5.12 b. Correlation plane pattern

5.4 RESULTS AND DISCUSSION

A set of simple holographic Optical Elements such as lenses, mirrors, gratings, complex matched spatial filters and multiple function HOEs are stimulated by using the experimental setup we have developed. A qualitative analysis of the performance of these HOEs has been done and was found to be satisfactory. Two optical frequency plane correlators have

been developed and the recognition peaks are obtained. The performance of these correlators are found comparable in their ability to recognize words.

The major feature of the latter frequency plane correlator system is the use of a converging reference beam. This enabled the recording of both the matched spatial filter and the transfer function of the Second Fourier transform lens in the same hologram and resulted in the reduction in size, weight, number of optical components necessary and the complexity of the system.

References

1. Gabor, D, Nature, 161, 777 (1948).
2. Gabor, D, Proc.Roy.Soc.A., 197, 454 (1949).
3. Gabor, D, Proc.Phys.Soc.B, 64, 449 (1951).
4. Rogers, G.L, Proc.Roy.Soc., 63A, 193 (1952).
5. Kock, W.E, Rosen, L and Rendeiro, Proc.IEEE, 54, 1599 (1966).
6. Schwar, M.J.R, Pandya, T.P and Weinberg, F.J, Nature 215, 239(1967).
7. Denisyuk, Yu. N, Opt.Spect., 15, 279 (1963).
8. Mintz, G.D, Morland, D.K and Boerner, W.M, Appl.Opt., 14, 564 (1975).
9. Gupta, P.C, and Aggarwal, A.K, Appl.Opt. 16, 1474 (1977).
10. Kogelnik, H, Appl.Opt. 11, 2426 (1972).
11. Gavrilov, G, Courjou, D and Buabois, J, Opt.Acta, 24, 837 (1977).
12. Kogelnik, H, Proc.Symp.on Modern Optics, p.605, Brooklyn, Polytechnic Press.
13. Murthy, M.V.R.K and Das, N.C, J.Opt.Soc.Am. 61, 1001, (1971).
14. Murthy, M.V.R.K and Das, N.C, J.Opt.Soc.Ind., 2. 53 (1973).
15. Hayat, G.S and Pieuchard, G, J.Opt.Soc.Am, 64, 1376 (1974)
16. Modyskin, Yu.S and Skrotskii, G.V, Sov.J.Quant.Electr. 2, 199 (1972).
17. Close, D.H, Opt.Engg. 14, 408 (1975).
18. Chang, B.J and Winick, K.A, Proc.SPIE, 299, 157 (1983).
19. Lerner, J.M, Flamand, J.F, Lande, J.P, Passereau, G and Thevenon, A, Proc.SPIE, 240, 82 (1980).
20. Ananda Rao, S and Pappu, S.V, Rev.Sci.Instrum., 51, 809, (1980).
21. Vander Lugt, A, IEEE Trans.Inform.Theory, IT-10, 139 (1964).

22.Andreas K.Richter and Paul Carlson, F, Appl.Opt. 13, 2924 (1974).

23.Mehta, P.C, Swami, S and Rampal, V.V, Appl.Opt., 16, 445 (1977).

24.Vilkomerson, D.H.R and Bostwick, D, Appl.Opt. 6, 1270 (1967).

25.Collier, R.J, Burckhardt, C.B and Lin, L.H, "Optical Holography, Academic Press, New York (1971).

26.Jose R.Magarinos and Daniel J.Coleman, Proc.SPIE, 523, 203 (1985).

27.Noda, H, Namioka, T and Seya, M, J.Opt.Soc.Am., 64, 1031,(1974).

28.Mahipal Singh, Ind. J Pure and Appl.Phy., 15, 338 (1977).

29.Syms, R.R.A and Solymer, L, Opt.Comm., 43, 107 (1982).

30.Syms, R.R.A and Solymer, L, Appl.Phys.B, 30, 177 (1983).

31.Neill, E.L.O, IRE Trans.Inform.Theory, IT-2. 56 (1956).

32.Vander Lugt, A, Appl.Opt., 5, 1760 (1966).

33.Vander Lugt, App.Opt. 6, 1221 (1967).

34.Casasent, D (Ed), "Topics in Applied Physics - Optical Data Processing", 23, Springer-Verlag, New York, (1978).

35.Casasent, D, Proc.IEEE, 67, 813 (1979).

36.Casasent, D, IEEE Spectrum, March, p.28. (1981).

37.Casasent, D, Opt.Engg. 24, 26 (1985).

38.Lahmann, A.W and Paris, D.P, Appl.Opt., 7, 651 (1968).

39.Binns, R.A, Dickinson, A and Watrasiewicz, B.M, Appl.Opt., 7, 1047 (1968).

40.Marck J.Bage and Michael P.Beddoes, App.Opt. 15, 2830,(1976)

41.Casasent, D and Alan Furman, Appl.Opt., 16, 1652 (1977).

42.Casasent, D and Alan Furman, Appl.Opt., 16, 1662 (1977).

43.Mehta, P.C ,Swami,S and Rampal,V,V,Appl.Opt.,16,445,(1977).

44.Ennis, J.D Jared, A.D, Opt.Engg., 25, 808 (1986).

45."Photonics Spectra", 20, 32 (1986).

46.Tien-Hsin Chao and Hua-Kuang Liu, Appl.Opt., 28, 226 (1989).

47.Vijayakumar, B.V.K, (Guest Editor), Opt.Engg., 29, (1990).

48.Shen M., Casasent, D, Luu, T.K and Feng, B, Opt.Comm., 34, 331,(1980).

49.Caulfield,(Ed.),"Handbook of Optical Holography" , Arsenault H.H, and Gilbert April, Academic Press, New York,Chapter 4,p 179, (1979).

50. Ezio Camtini (Ed.), "Optical and Acoustical Holography", Buschmann, H.T,153 (1972).

CHAPTER VI

CONCLUSIONS AND PROGNOSIS

CONCLUSIONS AND PROGNOSIS

In this work we have fabricated an indigenous,low cost holographic set up, which gives an all round performance within the domain of the demands and investment of a university research laboratory.The vibration analysis of a newly designed holographic table has been conducted. The performance of the table was found satisfactory for a table-top skin weight of 310kg. The good reconstructions of the holograms recorded at different environmental conditions and the stability of the fringes in real-time holographic experiments indicated the isolation capability of the table and its long-term usability.

A set of holders and positioners were designed and fabricated so as to satisfy the general and some special needs of holographic experiments.

Good quality optical components such as varying reflectivity beam-splitters, spatial-filters and beam directors were made by using the ingenious techniques developed in the laboratory and their performance was evaluated.

The entire cost of this holographic set up, excluding that of the laser and recording plates, was less than Rs.25,000.

A simple, sensitive and non-destructive method for the measurement of stress in reflecting thin films has been introduced by using real-time holographic interferometry . Thermal stress variation in reflecting Al, Cu and Ag films where studied by using the method. The stress values measured were found to be in good agreement with the theoretical stress values predicted. Other advantages of this technique over usual interferometric methods are that the fringes obtained are real and no substrate profile measurement is needed. In the present experiment we have studied the thermal stress variation in a temperature range of 20 to 100^{0}C and fringe ordering was measured with naked eye. The sensitivity of the method depends on the substrate thickness and resolution of the fringe read out system.For a film of 200 nm thickness on 0.015 cm thick glass plate the sensitivity was found to be 7×10^{6}dynes/cm^{2} and this is a fairly good value compared to other standard methods.

The variation of stress in thin films, for a higher temperature range, can be investigated with the help of thicker substrates and an automatic fringe read out system. The variation in the average stress due the variation of intrinsic stress with temperature may be evident in such experiments.

The capability of conventional holography to study the wall vibrations of an air-reed musical wind instrument, excited in an almost realistic playing conditions, has been demonstrated. A compressed air-ribbon has been used to excite a flute, even without touching it and without introducing any stability problems. The effect of the wall materials on the tone quality of a musical wind instrument has been investigated. It has been proved beyond doubt that the surface

vibrations in flutes made of reed are much greater than that of the metal flutes.This supports the rich sound of flutes made of reed, as claimed by the musicians.

We hope that if one can manage to collect a few great flutes with very good musical qualities, it would be possible by using this method to investigate the factors affecting the musical qualities and facilitate the design of consistently good instruments.

A few holographic optical elements were recorded by using the experimental set up and their performance was qualitatively analysed. We found that the diffraction efficiencies of these fabricated elements were not promising. This could be improved by varying the system parameters and by using recording materials with better diffraction efficiencies.

A compact setup for holographic pattern recognition was developed. The matched filter and the second Fourier transform lens were recorded in the same holographic plate. Good correlation peaks were obtained in the matched filter experiment.

A holographic matched filter of any simple object may be recorded and the performance of the filter can be compared to that of a computer generated holographic matched filter of the object. Positive results and practical realisation of such a system might be much military importance.With the availability of improved 2-D spatial light modulators, new correlation filter designs and interfacing hardware, a good amount of work on this area is progressing in different corners of the world.